7-2-2015 12:00 AM

Functional Characterization of P3N-PIPO Protein in the Potyviral Life Cycle

Hoda Yaghmaiean
The University of Western Ontario

Supervisor
Dr. Aiming Wang
The University of Western Ontario

Graduate Program in Biology
A thesis submitted in partial fulfillment of the requirements for the degree in Master of Science

FUNCTIONAL CHARACTERIZATION OF P3N-PIPO PROTEIN IN THE POTYVIRAL LIFE CYCLE

(Thesis format: Monograph)

by

Hoda Yaghmaiean

Graduate Program in Biology

A thesis submitted in partial fulfillment
of the requirements for the degree of
Master of Science

The School of Graduate and Postdoctoral Studies
The University of Western Ontario
London, Ontario, Canada

Abstract

Potyviruses represent the largest genus of plant-infecting viruses and include many agriculturally important viruses such as *Turnip mosaic virus* (TuMV), *Soybean mosaic virus* (SMV) and *Plum pox virus* (PPV). The potyviral genome consists of a large open reading frame (ORF) and a small ORF owing to a translational or transcriptional slippage in the P3 cistron. The polyproteins encoded by these two ORFs are proteolytically processed into 11 mature proteins. Recent studies have shown that P3N-PIPO, the frameshift resulting protein, is a plasmodesmata (PD)-located protein and involved in potyviral cell-to-cell movement by mediating the targeting of the potyviral CI protein to PD to form canonical structures for potyviral cell-to-cell movement. In this study, I introduced in a full-length cDNA infectious clone of TuMV a stop codon or point mutations into P3N-PIPO without affecting the amino acid sequence of other viral proteins including P3 and evaluated effects of these mutations on TuMV infection. It was found that elimination of PIPO or substitution of the positive charged amino acid lysine with the negatively charged amino acid glutamic acid within PIPO compromises TuMV cell-to-cell spreading in *Nicotiana benthamiana* plants. PEG-mediated transfection assay revealed that virus replication of these mutants is not affected in *Nicotiana benthamiana* protoplasts. Moreover, transient co-expression of CI and P3N-PIPO mutants showed that the PIPO mutants lose the ability to target the TuMV CI protein to plasmodesmata. Subcellular localization of these PIPO mutants indicated that the substitution mutants retain their PD-targeting. These data strongly support that the potyviral P3N-PIPO protein is likely a dedicated protein for potyviral intercellular movement via PD.

Keywords: Potyviruses, P3N-PIPO, TuMV, Intercellular movement, Plasmodesmata.

Acknowledgments

I would like to thank my supervisor, Dr. Aiming Wang, for his continuous patience and encouragement throughout my journey of obtaining my degree. I am especially grateful to him for giving me the opportunity to join his team to work on this project.

I am extremely grateful to my co-supervisor, Dr. Greg Thorn, for his valuable advice, assistance, and constructive suggestions on my project. I wish to thank my advisory committee Drs, Sashko Damjanovski and Krzysztof Szczyglowski for their helpful feedback.

I warmly thank the current and former members of the Wang lab. I wish to extend my warm appreciation to, Jamie McNeil, Alex Molnar, Dorothy Drew and Shelly Snook for their exceptional technical assistance at Southern Crop Protection and Food Research Centre, London, Ontario. I would like to express my gratitude to the staff of the University of Western Ontario especially Carol Curtis, Arzie Chant for all their help.

My deepest gratitude goes to my parents. I am indebted to their many sacrifices over the years in providing me the best possible studying opportunity and environment. Their high expectations have always motivated me to aim higher and work harder in accomplishing my goals. I also thank my two amazing brothers, for their good humor, understanding, and insightful counsels during my frustrating moments. Without doubt their support has strengthened and gave me the courage I needed to complete my studies.

Lastly, I would like to have a special thank you to my husband for all of his support and love and all the stolen moments from him during my study.

Table of Contents

List of Tables

List of Figures

List of Appendices

List of Abbreviations

BLAST	Basic Local Alignment Search Tool
Bp	base pair(s)
C	Centigrade
Cat #	Catalog Number
cDNA	Complimentary DNA
CDS	Coding DNA sequences
CFP	Cyan fluorescent protein
ddH2O	Double-distilled Water
DNA	Deoxyribonucleic acid
dNTP	Deoxyribonucleic triphosphates
E. coli	Escherichia coli
EtOH	Ethanol
G	Gravitational Force
GFP	Green Fluorescent Protein
h	Hour(s)
L	Liter(s)
LB	Luria Broth
M	Molar
mg	Milligram(s)
mM	Millimolar(s)
mL	Milliliter(s)
NaCl	Sodium Chloride
OD 600	Optical density at 600 nm
PCR	Polymerase Chain Reaction
PEG	Polyethylene glycol
qPCR	Quantitative PCR
qRT-PCR	Reverse Transcription qPCR
RNA	Ribonucleic acid
RT	Room Temperature

SDS	Sodium Dodecyl Sulphate
TBE	Tris/Borate/EDTA Buffer
TAE	Tris-acetate-EDTA
Tris	Tris-(hydroxylmethyl)-methylamine
U	Unit
UV	Ultra-violet
Vol	Volume
w/v	Weight/volume
μL	Microliter(s)
μg	Microgram(s)
YFP	Yellow fluorescent protein

Chapter 1

1 Introduction

1.1 General background about plant viruses

Plant viruses are grouped into 73 genera and 49 families (Hull, 2013). Like all other viruses, plant viruses are intracellular parasites that can replicated only inside living cells (Matthews and Hull, 2002; Hipper et al., 2013). All viruses have a very small genome that encodes a limited number of proteins, and thus depend on host factors for viral multiplication (Ahlquist et al., 2003; Laliberté and Sanfaçon, 2010). Viruses maintain very basic fundamental structures and limited properties but can display a great adaptability in different habitats by genetic variability over time (Thresh, 2006). Viruses are extremely small and can only be observed under an electron microscope. The simplest viruses are composed of a small piece of nucleic acid (DNA/RNA) surrounded by a coat protein (Ahlquist et al., 2003). Only a minority of plant viruses possess double-stranded DNA (dsDNA) genomes, and some have genomes composed of single-stranded (ss) DNA. However, the genomes of most plant viruses are composed of RNA. Most of these genomes are composed of ssRNA that is the same (positive-sense) polarity as the messenger RNAs of the cell (Laliberté and Sanfaçon, 2010; Hull, 2013). All types of living organisms, including plants, animals, fungi, and bacteria are hosts for viruses, but most viruses infect only one type of host. In the case of plant viruses, differences in host range and susceptibility or response of plants to infection suggest that viruses can act as selective pathogens between species in natural plants. To transmit from one plant cell to another, plant viruses must use strategies that are usually different from animal viruses.

Plants do not move, and so plant-to-plant transmission usually involves vectors such as insects (e.g., aphids) or mechanical inoculation (Ivanov et al., 2014). Plant viruses cause many important plant diseases and are responsible for losses in crop yield and quality around the world (Gergerich and Dolja, 2006). In addition, infection by plant viruses can cause a variety of symptoms in hosts, such as stunted growth, yellowing, ring spot (chlorotic or necrotic rings) or necrosis on different parts of the plants tissue (Matthews and Hull, 2002). Plant virology as a subject of study started in the late nineteenth century, when Dutch microbiologist Martinus Beijerinc*k* and Russian researcher Dmitrii Iwanowski were studying the reason behind a mysterious disease of tobacco. *Tobacco mosaic virus* (TMV) was the first virus to be discovered over a century ago and was the first virus ever purified. Since then, over 1000 species of plant viruses have been identified (Scholthof, 2008).

1.2 The family *Potyviridae*

1.2.1 General description of *Potyviridae*

Potyviridae are very important as pathogens globally due to the great economic losses in crops caused by this family. Viruses in this family have also drawn the attention of the research community for years, and much effort has been made to study taxonomy, evolution, structure, functional characterization of viral proteins, diagnosis, control and interaction with hosts (López-Moya et al., 2009). These types of research have resulted in positive steps for controlling virus propagation and designing antiviral strategies. The *Potyviridae* comprise more than 30% of known plant virus species (Fauquet et al., 2005). *Potyvirus*, the major genus in the *Potyviridae* family, includes many agriculturally

important viruses such as *Plum pox virus* (PPV), *Potato virus Y* (PVY), *Potato virus A* (PVA), *Papaya ringspot virus* (PRSV), *Zucchini yellow mosaic virus* (ZYMV), *Bean common mosaic virus* (BCMV), *Maize dwarf mosaic virus* (MDMV), *Turnip mosaic virus* (TuMV), *Tobacco etch virus* (TEV), *Lettuce mosaic virus* (LMV) and *Soybean mosaic virus* (SMV). The genus is named after the type virus *Potato virus Y,* and, based on the genome organization, belongs to the picorna-like viruses superfamily (Urcuqui-Inchima et al., 2001; Wei et al., 2010; King et al., 2012). Potyviruses are flexuous, rod-shaped particles 680-900 nm long and 11-15 nm wide. They are composed of a single positive stranded RNA around 10 kb long which is surrounded with a protein shell known as a capsid, but lack a lipid bilayer (envelope). The capsid is made of approximately 2000 units of a single virally encoded protein, the capsid protein (CP). Potyviruses are transmitted predominantly by aphids in a non-persistent manner (Urcuqui-Inchima et al., 2001; Walsh and Jenner, 2002).

1.2.2 Genomic organization of potyviruses

The genomic RNA of potyviruses has a poly-adenine (A) tail of variable length at its 3' end and a VPg (viral protein genome linked) covalently bound to its 5' end. The genome codes for a long open reading frame (ORF) flanked by two untranslated regions (UTRs) (Majer et al., 2014) and also a small ORF owing to a translational or transcriptional slippage in the P3 cistron (Chung et al., 2008; Rodamilans et al., 2015). The two polyproteins encoded by the virus are processed co- and post-translationally by three viral encoded proteases (P1, HC-Pro, NIa-Pro) to generate 11 mature protein products (Chung et al., 2008; Wei et al., 2010). These viral proteins are, from the N to C terminus of the poly protein: P1 (the first protein), HC-Pro (the helper component/protease), P3 (the third

protein), P3N-PIPO (resulting from the frame-shift in the P3 cistron), 6K1 (the first 6 kDa peptide), CI (the cylindrical inclusion protein), 6K2 (the second 6 kDa peptide), NIa-VPg (nuclear inclusion ‘a’ – viral genome-linked protein; also VPg), NIa-Pro (nuclear inclusion ‘a’ protein – the protease), NIb (the nuclear inclusion ‘b’ protein), and CP (coat protein) (Riechmann et al., 1992; Urcuqui-Inchima et al., 2001; Wei et al., 2010).

1.2.3 Overview of potyviral functions

The first protein, P1, is a proteinase. P1 is a type of serine proteinase that self-cleaves the P1/HC-PRO junction at a specific conserved motif (Adams et al., 2005; Tena Fernández et al., 2013). The P1 protein has shown the ability to bind nonspecifically to RNA (Urcuqui-Inchima et al., 2001; Tena Fernández et al., 2013). P1 is also involved in host defense suppression. It was shown that the fusion of P1 and HC-Pro enhances viral pathogenicity through suppression of post-transcriptional gene silencing (PTGS) in the plant cells (Syller, 2006; Tena Fernández et al., 2013). HC-Pro is a multifunctional protein and is involved in various steps of the viral life cycle such as interaction with aphids and virus particles (Roudet-Tavert et al., 2002), self-interaction, amplification and systemic movement (Syller, 2006; Torres-Barceló et al., 2010; Hipper et al., 2013), synergism, symptom development and suppression of gene silencing (Mallory et al., 2001). The P3 protein and P1 together are the most variable proteins in this family (Urcuqui-Inchima et al., 2001). The P3 protein plays a vital role in pathogenicity through interaction with other potyviral proteins (Saenz et al., 2000). CI is an important protein for viral replication. The N-terminal segment of this protein contains several conserved motifs which are involved in (nucleoside-triphosphate) NTP binding, NTPase, RNA

binding, and RNA helicase activity (Urcuqui-Inchima et al., 2001; Sorel et al., 2014). It was proposed that the 6k1 protein carries a determinant for pathogenicity. 6k2 is required for inducing the formation of viral replication vesicles (Grangeon et al., 2013). NIa is divided into two domains based on functions, the N-terminal VPg domain, and the C-terminal proteinase domain. NIa is the major proteinase of Potyviruses: it processes the polyprotein in *cis* and in *trans* to produce functional products(Jebasingh et al., 2013). NIa-VPg (N-terminal part of NIa) is referred to as VPg protein, which is involved in viral genome replication and movement (Urcuqui-Inchima et al., 2001). RNA polymerase II (RdRp) that can produce complementary viral RNA during the replication process. The Glycine–Asparagine–Asparagine (GDD) motif is a highly conserved motif that is located in this protein, and -deletion or mutation of GDD is lethal to the virus (Riechmann et al., 1992; Urcuqui-Inchima et al., 2001). CP is involved in the protection of viral genomes, systemic movement and aphid transmission (Blanc et al., 1997; Fernandez-Fernandez et al., 2002). The recently discovered protein PIPO (pretty interesting *potyviridae* ORF) is produced by +2 frameshifting in the P3 cistron. The possible roles of this protein include cell-to-cell movement and replication or combinations of those functions (Chung et al., 2008).

1.2.4 Overlapping essential PIPO gene in the *Potyviridae*

Based on bioinformatics results by MLOGD gene-finding software, Chung et al. (2008) suggested that the high conserved motif (G2A6) at the 5 ´ end of PIPO frame facilitates ribosomal frame shifting. In addition to that they revealed that the PIPO ORF (+2 frame relative to polyprotein) is present in all 48 potyviral genome sequences in Genbank

(Chung et al., 2008). The length of PIPO is quite variable among the different potyvirus species, ranging from 60 to 115 codons and this variability in length was associated with the host species, geographic province or other strain features (Hillung et al., 2013). Previously Chung et al. (2008) and Vijayapalani et al. (2012), presented evidence indicating that detection of 7 kDa PIPO protein was not successful in TuMV infected tissues and instead a 25 kDa protein product, consistent with the predicted size for the fusion protein of the N-terminal region (upstream of the frameshift site) and PIPO, was detected. More recently, study by Rodamilans et al. (2015) suggested that P3N-PIPO is produced at least partially through polymerase slippage. They also mentioned that this possibility, previously considered by Chung et al. could not be demonstrated at that time likely due to the low rate of nucleotide insertion in this site. Therefore, P3N-PIPO was chosen for this study.

1.2.5 General life cycle of *Potyvirus*

The main steps of the *Potyvirus* life cycle are entry, decoating, translation, replication, assembly, cell-to-cell and systemic movement and plant to plant transmission (Ivanov et al., 2014). The *Potyvirus* genome is expressed as a polyprotein which is processed into eleven mature proteins. The majority of these proteins are multifunctional proteins although most of the viral proteins are involved in some way in viral replication (Matthews and Hull, 2002). Initially, the virus penetrates a host cell by insect vector or mechanical transmission then uncoats and viral genomic RNAs are released from the virions into the host cytoplasm and act as templates for translation to produce viral proteins (which is processed by viral proteases) using the host's translation machinery (Dreher and Miller, 2006; Simon and Miller, 2013). The viral replicase proteins associate

with cellular membranes where host factors are recruited to form the viral replication complex (VRC). Viral multiplication is carried out by the membrane bound VRC. The VRC synthesizes a complementary negative-strand RNA [(-)RNA] using the original genomic RNA as a template. The (-)RNA is then used as a template to synthesize many new (+)RNAs that undergo more rounds of translation and replication, or move to adjacent cells, or are encapsidated into virions. In the next step, viral cell-to-cell movement via plasmodesmata (PD) and formation of PD-associated pinwheel structures by viral proteins are followed (Wei et al., 2010; Nagy and Pogany, 2012) (Fig. 1.1). For long-distance, virus must move from the mesophyll via bundle sheath cells, phloem parenchyma, and companion cells into phloem sieve elements (SEs), and are then passively transported following the source-to-sink flow of photo assimilates and unloaded from SEs to sink tissues (distant sites) from which further infection will occur (Hipper et al., 2013).

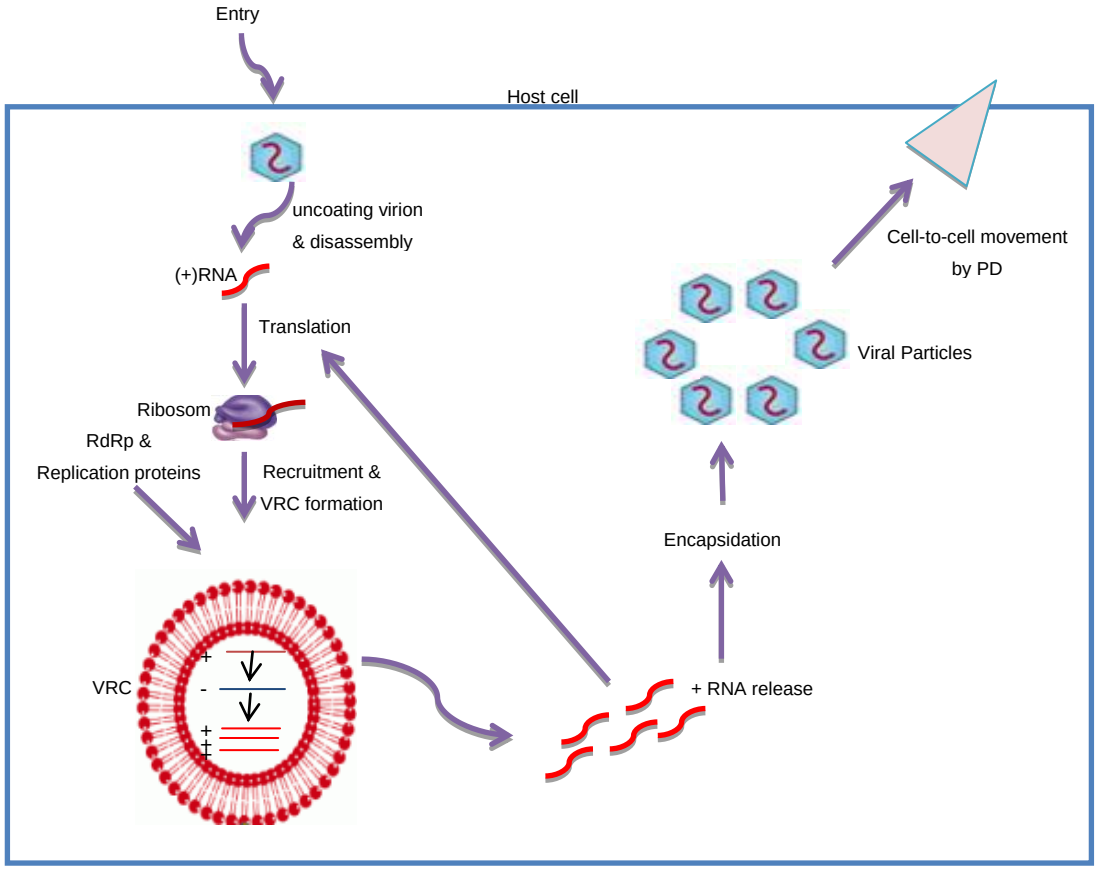

Figure 1.1 Schematic infection cycle of positive-sense RNA viruses. Virion enters the plant cells by insect vector. Following virion uncoating, potyviral RNA is translated by host cell ribosomes into polyprotein. The resulting viral replication proteins then recruit the (+)RNA to membranous vesicles, where functional viral replication complexes (VRCs) are assembled. A small amount of negative-sense RNA ((−)RNA) is synthesized and serves as a template for the synthesis of a large number of (+)RNA progeny. The new (+)RNAs are released from the VRCs, whereas the (−)RNA is retained. The released (+)RNAs start a new cycle of translation and replication, become encapsidated, and then exit the cells move to neighboring cells through plasmodesmata.

1.2.6 *Potyvirus* movement

The movement of viruses in plants is divided into three steps: intracellular, intercellular and long distance movement (Nelson and Citovsky, 2005; Benitez-Alfonso et al., 2010). Initially, the virus moves intracellularly from the sites of replication to plasmodesmata (PD). PD are a unique intercellular membranous channel which can control the intercellular trafficking of micro- and macro- molecules, including plant viruses. This complicated structure also establishes cytoplasmic and endomembrane continuity between neighboring cells (Oparka, 2004). The virus further transverses the PD to spread intercellularly (cell-to-cell movement). Finally, long distance movement of the virus within the plant happens through phloem sieve tubes and xylem. The plant to plant transmission happened by aphids (Boevink and Oparka, 2005; Lucas, 2006).

Viral cell-to-cell movement through PD is mediated by virus-encoded factors termed movement protein (MP) (Heinlein, 2015). The first evidence demonstrating that the process of plant virus movement is controlled by certain viral proteins came from early investigations of temperature sensitive mutants of TMV encoding a nonstructural 30 kDa MP (Taliansky et al., 2008; Harries and Ding, 2011).

Plant viruses can be classified into several groups based on the characteristics of their intercellular transport. One group, which includes TMV and related viruses, encodes a single dedicated MP that associates with, and increases the size exclusion limits of, PD to allow transport of viral genomes through the modified channel (van Regenmortel et al., 2000; Ohshima et al., 2002). The second group includes many plant viruses with icosahedral particles, and requires both the MP and CP for cell-to-cell movement (Ohshima et al., 2002). The third group includes several viruses with filamentous

particles, such as *Potexviruses*, that contain a set of three movement genes called the triple gene block. These genes encode proteins that are assumed to function coordinately, but without forming the tubular structure, to transport viral particles or genomes through PD (Heinlein, 2015). In the case of *Potyvirus*, no dedicated MP, like those for other viruses, has been identified. However, some potyviral proteins, including HC-Pro, CI, VPg, CP, and P3N-PIPO, have been demonstrated to be involved in viral cell-to-cell movement (Dunoyer et al., 2004; Hofius et al., 2007; Wei et al., 2010; Vijayapalani et al., 2012; Ivanov et al., 2014)..

1.3 TuMV

1.3.1 Taxonomy and genome organization

TuMV was ranked the second most important virus infecting field-grown vegetables. Like other viruses in this genus, TuMV is transmitted by aphids (van Regenmortel et al., 2000). This family, belonging to the picorna-like virus super group, includes plant and animal viruses (Culley et al., 2003). Seventy-six isolates of TuMV were collected from around the world, mostly from *Brassica* and *Raphanus* crops, but also from several non-brassica species (Ohshima et al., 2002). TuMV virions are non-enveloped, flexuous rod-shaped particles of ~720 nm long and 15-20 nm wide (Walsh and Jenner, 2002) (Fig. 1.2). The TuMV genomic RNA is 9830 nucleotides in length. The molecular mass of viral proteins is P1 (40 kDa), HC-Pro (52 kDa), P3 (40 kDa), P3N-PIPO (25 kDa), 6K1 (6 kDa), CI protein (72 kDa), 6K2 (6 kDa), VPg protein (22 kDa), NIa (27 kDa), NIb (60 kDa) and the CP (33 kDa) as shown in (Fig. 1.2) (Walsh and Jenner, 2002; Chung et al., 2008; Wei et al., 2010). An infectious clone of TuMV has been produced, providing a

tool of enormous potential to study the molecular genetics of TuMV (Sánchez et al., 1998).

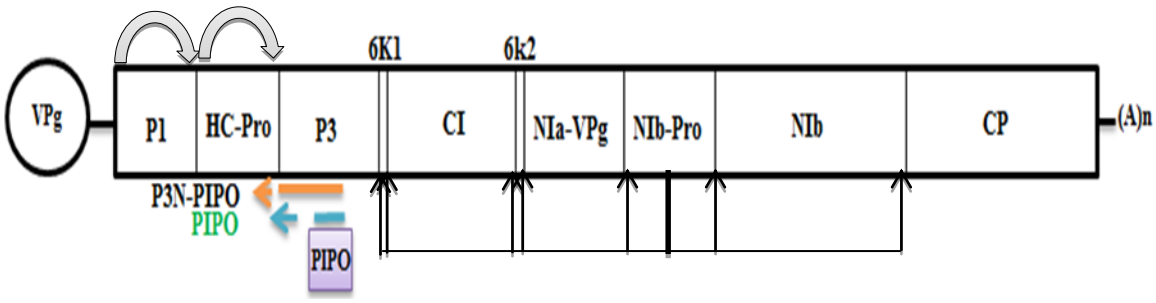

Figure 1.2 Schematic representation of TuMV genome. The viral RNA is symbolized by the horizontal line, linked to a single VPg at the 5′ end and to a poly (A) tail at the 3′ end. The poly protein is processed by three different proteinases to 11 mature proteins. The black arrows indicate the cleavage site. P3N-PIPO results from the translation of the 5′ sequence of TuMV P3 cistron followed by a small open reading frame protein embedded in the cistron. The arrows indicated the place of proteinase cleavage.

1.3.2 Host range and transmission

The wide host range of TuMV is one of its remarkable features. At least 318 species of plants including both dicots and monocots, in more than 43 families, are known to be infected by TuMV (Walsh and Jenner, 2002). TuMV is known to be particularly damaging in brassicas (members of the mustard family or *Brassicaceae*) in parts of Asia, North America and Europe. It has caused serious losses in arable crops, including oilseed rape (*Brassica napus*) and vegetable crops, including swede/rutabaga (*B. napus*), turnip, Chinese cabbage (*B. rapa*), cabbage, Brussel sprouts, cauliflower, kohlrabi and collards (*B. oleracea*) (Nguyen et al., 2013). It also infects and causes damage in many non-brassica crops and ornamentals, including radish, lettuce, endive, escarole, horseradish, peas, courgette, rhubarb, statice (*Limonium*) and stock (*Matthiola*) (Walsh and Jenner, 2002). TuMV occurs in many parts of the world, including the temperate and tropical regions of Africa, Asia, Oceania and North and South America (Nguyen et al., 2013). This virus is transmitted to plants through 40-50 species of aphids in a non-persistent manner.

1.3.3 Disease symptoms

TuMV infection results in different symptoms depending on the plant, such as mosaic, mottling, chlorotic rings or color break on stems, foliage, flowers and fruits. The infection can also cause severe stunting of young plants and represents an important reduction of yield. Malformations of leaf, stem and fruit can also be observed as well as fruit drop and necrosis of different tissues (Shukla et al., 1994) (Fig. 1.3).

Figure 1.3 Turnip mosaic virus symptoms on a cabbage leaf of the variety Superdane. Photo courtesy of T.A. Zitter, Cornell University, Ithaca, NY.

1.4 Proposed research

Viruses are considered one of the major constraints to agricultural production in the world. A better understanding of the molecular biology of viruses and the functions of the viral proteins is essential for the control of virus propagation and the elaboration of antiviral strategies. For example, viral disease may be controlled by disruption of viral cell-to-cell movement. Previously our lab (Wei et al., 2010) showed that the potyviral protein P3N-PIPO is a PD-located protein and directs the CI protein to PD, facilitating the deposition of the cone-shaped structures of CI at the PD by interacting with the CI protein. Therefore, CI and P3N-PIPO coordinate the formation of conical structures at PD for potyviral cell-to-cell spread (Wei et al., 2010). However, it is not clear how P3N-PIPO directs CI targeting to the PD, if P3N-PIPO is directly involved in viral cell-to-cell movement and if P3N-PIPO is also involved in other steps of the viral cycle. This project aims to further characterize the functional role of the P3N-PIPO protein of TuMV using a pCambiaTunosGFP infectious clone containing the full-length cDNA of TuMV with GFP inserted at the junction between the P1 and HC-Pro protein. Our general research hypothesis is that like other potyviral proteins, the PIPO protein of TuMV plays multiple roles in viral infection. Therefore, site-directed mutants in PIPO without alteration of P3N or P3 amino acid sequences will provide evidence of PIPO role in the virus life cycle. The objectives of this project are as follows:

1. To generate P3N-PIPO mutants

   To explore the functional roles of P3N-PIPO, the recombinant TuMV infectious clone tagged by GFP has been used to generate various P3N-PIPO mutants. Since the

N-terminal region, i.e., P3N, of P3N-PIPO is also part of the P3 protein; I only mutated the C-terminal region, i.e., PIPO, of P3N-PIPO.

2. To evaluate cell-to-cell movement of TuMV mutants in which P3N-PIPO is mutated.

   Transient expression of PIPO mutants in *Nicotiana benthamiana* has been used for evaluation of cell-to-cell movement. Constructed mutant plasmids were transformed in *Agrobacterium tumefaciens* strain GV310. Plants were agroinfiltrated with appropriate agrobacterial cultures and the agroinfiltrated plants were maintained under normal growth conditions for 14 days and then examined using confocal microscopy.

3. To evaluate long distance movement of TuMV mutants in which P3N-PIPO is mutated

   Newly emerging leaves (new leaves which are located above the level of the inoculated leaves and can acquire infection from inoculated leaves after infiltration) were examined for GFP localization under UV light after 14 days post inoculation.

4. To subcellularly co-localize the P3N-PIPO mutated version with CI

   To determine if PIPO mutants can interact with the CI protein, I coexpressed the CI protein and P3N-PIPO mutants with different fluorescent tags, such as cyan fluorescence protein (CFP) and yellow fluorescence protein (YFP). The inoculated leaves with those plasmids were examined using confocal microscopy.

5. To conduct a replication assay

   To study if the PIPO protein has any effect in replication, I examined the constructed PIPO mutants with respect to replication in protoplasts. PEG-mediated transfection was used to deliver mutant virus infectious plasmids into protoplasts and these were

studied using confocal microscopy. Total RNA was extracted from the protoplasts, followed by real time RT-PCR with specific TuMV CP primers.

6. To determine possible interactions of CI and P3N-PIPO

Constructs used for the expression of the punctate forms of CI in PD were prepared based on their predicted conserved domain structure. For this purpose, I divided the CI protein into the desired size of fragments and examined those fragments using two systems, bimolecular fluorescence complementation assay (BIFC) in planta and Y2H screen in yeast.

Chapter 2

2 Material and method

2.1 Plant material and growth conditions

Nicotiana benthamiana plants were cultivated in a growth room at 16 hours in the light at 24 °C and then 8 hours in the dark at 21 °C with 75% relative humidity. Four-to-five-week-old plants were used for infiltration with *Agrobacterium tumefaciens* strain (GV1301) harboring appropriate plant expression vectors. For protoplast isolation from leaf cells, *Nicotiana benthamiana* plants were kept in a Percival growth chamber (Johns Scientific Inc., Canada) with a different photoperiod of 16 hours of darkness at 22 °C and 8 hour of light at 20 °C (Wu et al., 2009).

2.2 General molecular biology techniques

General lab and molecular techniques essentially followed those in *Molecular Cloning: A Laboratory Manual* (Sambrook and Russell, 2006) unless otherwise stated.

2.2.1 Bacterial strain and cultures

In this study *Escherichia coli* DH5α or DH10B was used for cell transformation and *Agrobacterium tumefaciens* GV3101 was used for plant transformation. The bacteria or agrobacteria were cultured at 37 °C in Luria-Bertani (LB) broth [1% tryptone, 1% NaCl, 0.5% yeast extract] or on LB agar plates (with 1.5% w/v agar). The LB media contained 50 μg mL^{-1} of kanamycin which was selective for the desired plasmids in this work. In addition to the kanamycin antibiotic the *Agrobacterium* culture media also contained 50 μg mL^{-1} of rifampicin and gentamicin antibiotics. For long-term storage, 600 μL of

overnight LB culture containing the appropriate antibiotics, was mixed with 400 µL of 50% glycerol and kept in the -80 ºC freezer.

2.2.2 Antibiotic stock preparation

An antibiotic stock concentration of 100 mg/mL was used. For this purpose the powder was dissolved in miliiQ water (e.g. 1 g powder in 10 mL H_2O), and was then sterilized through a 0.22 µm pore size filter. In the case of rifampicin the antibiotic powder was dissolved in methanol as a solvent. The aliquots were stored at -20 ºC. It was necessary to cool the LB medium before adding antibiotics as the heat could inactive them. In order to do this, the autoclaved medium was equilibrated in a water bath set at 55-60 ºC for a minimum of 30 min, and then the desired antibiotics was added.

2.2.3 Preparation of *E.coli* competent cells

A colony from a freshly streaked *E. coli* (DH10B) was used for inocula tion in 5 ml of liquid LB medium and this inoculum allowed grown at in 37 °C with shaking at 200 rpm overnight. 500 µL of overnight culture was added to 50 mL of fresh liquid LB medium and placed at 37 °C in a shaker for 2-3 hours. OD_{600} was measured on an hourly basis until it reached 0.3-0.4 optical density. The cells were harvested by centrifugation at 3000 rpm for 10 min at 4 °C. The pellet was gently resuspended in 30 mL of pre-chilled transformation buffer (0.1 M $CaCl_2$, 1 M $MgCl_2$) and the cells were incubated on ice for 30 min and then centrifuged at 3000 rpm at 4 °C for 10 min. The supernatant was discarded and the pellet was resuspended in 1 mL of pre-chilled resuspension solution

(0.1 M $CaCl_2$, 80% glycerol). The suspension was aliquoted in sterile eppendorf tubes. The cells aliquots were kept in a -80 °C freezer for long term storage.

2.2.4 Preparation of *Agrobacterium tumefaciens* competent cells

A colony from a freshly streaked *Agrobacterium tumefaciens* GV3101 was used to inoculate 100 mL of LB medium with appropriate antibiotics (50 μg mL^{-1} of gentamicin and rifampicin). The flask was incubated at 30 °C with vigorous shaking for overnight. The agrobacterial cells were washed three times by spinning at 5000 rpm for 5 min at 4 °C and resuspended in 50 mL ice cold 10% glycerol. After washing, the agrobacterial pellet were resuspend in 1 mL of 10% glycerol. Aliquots of 40 μL of the *Agrobacterium* competent cells were transferred to Eppendorf tubes and placed in a -80 °C freezer for long term storage.

2.2.5 Gel electroprosis and DNA isolation

Plasmid DNA and DNA fragments were separated on 1% agarose gels which were prepared with a 1X (TAE) buffer (2 mM EDTA, 40 mM Tris-acetate) at pH 8.0. Ethidium bromide (0.5 μg mL^{-1}) was added to the gel before solidification. DNA samples or PCR reactions were loaded with 1X loading dye and gels were run at 150 V. Gels were studied using a UV trans-illuminator. For cloning, the gel containing DNA fragments were sliced and the DNA fragments were isolated from the gel using the QIAquick Gel Extraction Kit (Qiagen) according to the manufacturer's manual.

2.2.6 Restriction enzyme digestion

Two μg of plasmids were digested with appropriate restriction enzymes (such as SnaBI and KpnI) in 15μl reaction mixtures with specific enzyme buffers. Reactions were incubated at 37 ºC for 1-1.5 hours then the whole mixture was separated on 1% agarose gels for 30 min. The desired fragments were isolated using the QIAquick Gel Extraction Kit.

2.2.7 Bacterial transformation

All bacterial transformations were performed by the heat shock method as recommended in the Invitrogen (Life Technologies) user guide. The plasmid DNA was gently added to 50 μL of DH10B competent cells and the reaction was incubated on ice for 30 min. The cells were heat shocked at 42 ºC for 45 seconds and transferred to ice for about 2 min. 250 μL of fresh LB medium was added to the reaction and incubated for 1 hour at 37 ºC, then the culture spread on LB agar plates supplemented with appropriate antibiotic and incubated at 37 ºC overnight.

2.2.8 Transformation of *Agrobacterium tumefaciens* by electroporation

Plasmid DNA (50-200 ng) was gently added to 40 μL *Agrobacterium* competent cells. The mixture was transferred into a pre-chilled electroporation Gene Pulser® cuvettes (Bio-Rad) with 2mm separation. The cells were pulsed with Bio-Rad MicroPulserset at 1.8 kV and recovered immediately in 1 mL of fresh LB medium and allowed to grow in 28 °C with vigorous shaking for 1-2 hours, and then 20 μL of culture was plated on an

LB agar plate supplemented with appropriate antibiotics. The plates were incubated at 28 °C for 2-3 days.

2.2.9 DNA sequencing

DNA Sanger sequencing was done by DNA sequencing facility by using applied biosystem AB3100XC at the Southern Crop Protection and Food Research Center, Agriculture and Agri-Food Canada, London, Ontario.

2.3 TuMV PIPO protein-coding region

To functionally characterize P3N-PIPO, the vector pCambiaTunos/GFP infectious clone which contains the full-length cDNA of TuMV (Cotton et al., 2009) was used to generate various PIPO mutants (Fig. 2.1 B). Since the N-terminal region, i.e., P3N, of P3N-PIPO is also part of the P3 protein, I only mutated the C-terminal region, i.e., PIPO, of P3N-PIPO. Previously Chung et al. (Chung et al., 2008) analyzed 48 potyvirus sequences including TuMV strain UK1 (Gene bank accession NC-002509) and predicted that TuMV PIPO is 60 amino acid in length and is encoded by the nucleotide sequence 3079-3258. Based on this information, the codon AAA (3079-3081) encoding Lysine is the first amino acid of the PIPO.

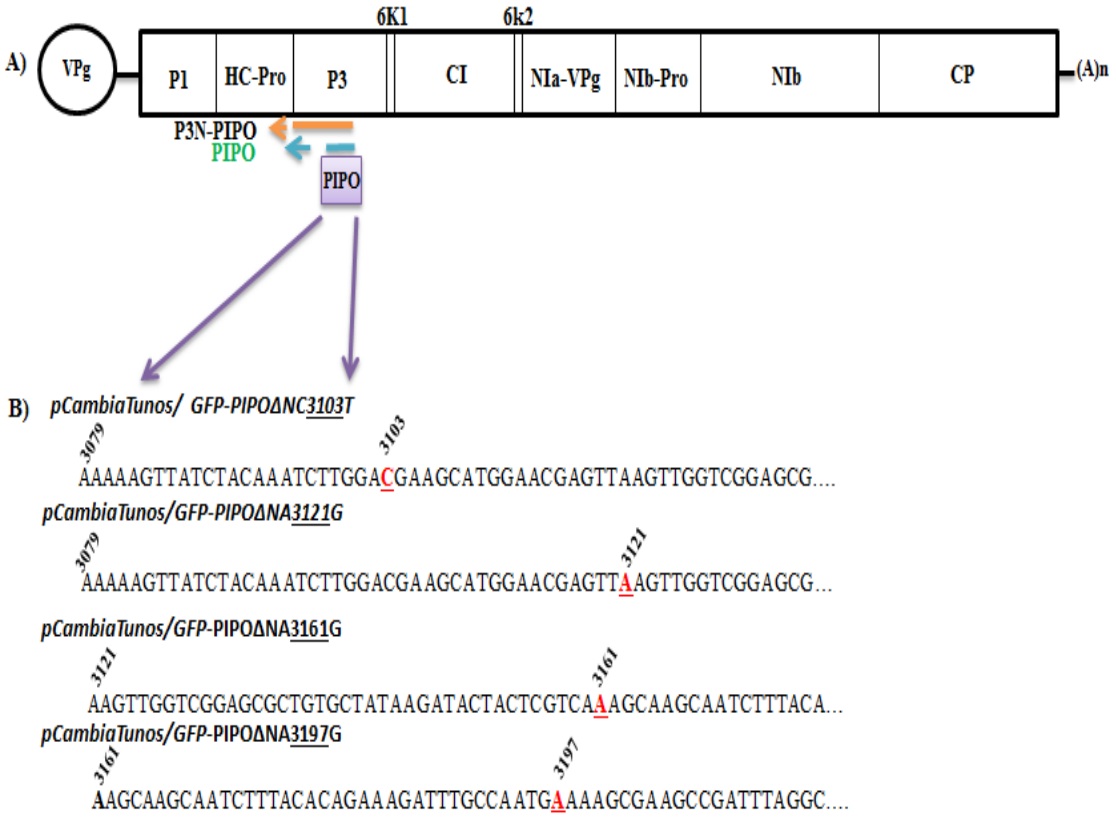

Figure 2.1 Schematic representation of the TuMV genome. The viral RNA is symbolized by the horizontal line, linked to a single VPg at 5□ end and to a poly (A) tail at the 3□ end. Two polyproteins are processed by three different proteinases into 11 mature proteins. Of them, P3N-PIPO, resulting from the translation of the 5□ sequence of TuMV P3 cistron is followed by a small open reading frame protein embedded in the cistron (A). Different PIPO mutants were created in cDNA, an infectious clone of TuMV (pCambiaTunos/GFP) which is GFP fused between P1 and HC-Pro. Red letters within the PIPO sequences indicates the location of the introduced mutation (B).

2.4 Plasmid construction for PIPO mutants

All PIPO mutant constructs were obtained by overlapping PCR using Phusion™ High-Fidelity DNA Polymerase® (Fermentas). Mutations were introduced into the full-length cDNA infectious clone of TuMV (pCambiaTunosGFP) strain UK1 (Gene bank accession NC-002509) (Cotton et al., 2009). Mutagenic primers for specific positions are shown in Table 2.1. All of the primers in this study were designed using Lasergene 10 software. In the first step, two pairs of primers were used to generate DNA fragments with overlapping ends containing the desired mutation. These two DNA fragments were then mixed and annealed to get hybrid duplexes. In the second step, the resulting hybrids were then extended and amplified to yield recombined PCR products that could be directly cloned into an appropriate plasmid vector following restricted digestion (Tomlinson, 1987) (Fig. 2.1). The amplified products were purified from agarose gels by QIAquick Gel Extraction Kit (Qiagen). The PCR product was ligated into the pCR™-Blunt vector (Invitrogen) and then transformed by heat shock to *E.Coli* DH5α strain according to the manufacturer's manual (Invitrogen). Single colonies were used to inoculate 3 mL of LB medium with appropriate antibiotics and grown overnight at 37 ºC. Plasmid extraction was performed for each culture by QIAprep Spin Miniprep Kit (Qiagen). Digestion was performed with appropriate restriction enzymes SnaBI and KpnI (NEB). The desired fragment was inserted back into the corresponding restriction sites of the parental infectious clone (pCambiaTunosGFP). The modified plasmid was confirmed by DNA sequencing (Shukla et al., 1994).

Table 2.1 Mutagenic Primers for PIPO mutants and plasmid construction.

Gene ID	Primer Sequence (5′ to 3′)	Target gene
P3-FW	GGGGTACCAAATGGGTCACGGAAA	*P3*
P3-REV	CGC CGGTACGTAATCTAT TACCTATA	*P3*
PIPO(R9St)-FW	ACAAATCTTGGATGAAGCATGGAACGA	*PIPO*
PIPO(R9St)-REV	TCGTTCCATGCTTCATCCAAGATTTGT	*PIPO*
PIPO(K15E)-FW	ATGGAACGAGTTGAGTTGGTCGGAGCG	*PIPO*
PIPO(K15E)-REV	CGCTCCGACCAACTCAACTCGTTCCAT	*PIPO*
PIPO(K28E)-FW	ATACTACTCGTCGAAGCAAGCAATCTT	*PIPO*
PIPO(K28E)-REV	AAGATTGCTTGCTTCGACGAGTAGTAT	*PIPO*
PIPO(K41E)-FW	TTTGCCAATGAAGAGCGAAGCCGATTT	*PIPO*
PIPO(K41E)-REV	AAATCGGCTTCGCTCTTCATTGGCAAA	*PIPO*

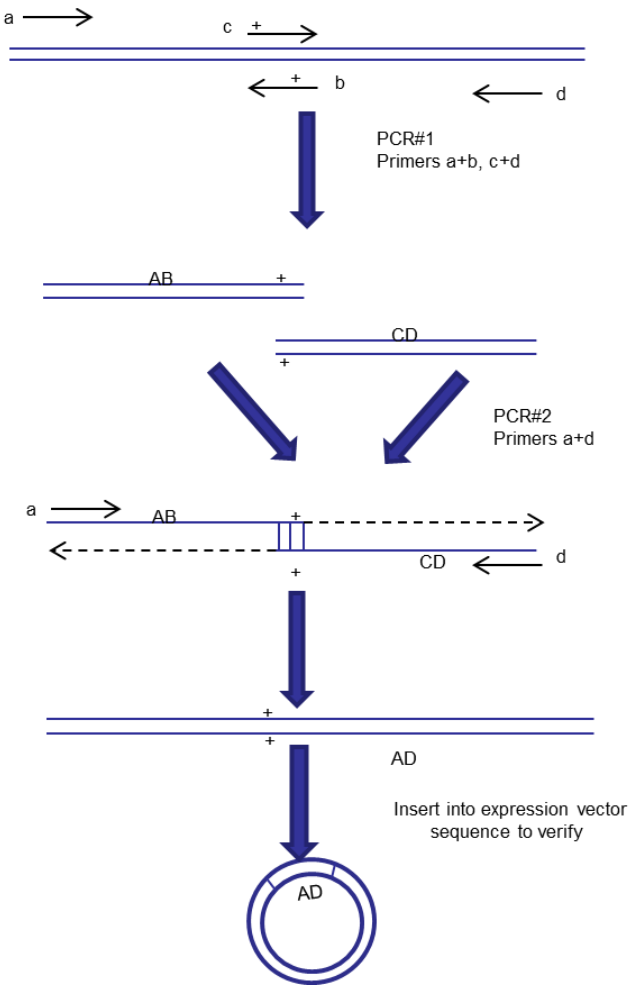

Figure 2.2 Schematic representation of overlapping PCR. Overlapping PCR was used to create specific nucleotide mutations or generate chimeric gene products. The AB segment is amplified using primers a and b, and the CD segment is produced with primers c and d. The PCR products AB and CD are the two overlapping fragments of AD. AD can be obtained using AB and CD as template and primers a and d.

2.5 Transient expression in *Nicotiana benthamiana*

Plant expression vectors were transformed by electroporation into *Agrobacterium tumefaciens* strain GV3101. For agroinfiltration, agrobacterial cultures were grown overnight in LB medium containing appropriate antibiotics. Cells were collected by centrifugation at 4500 rpm for 3 min at room temperature (RT), and the pellet resuspended in an infiltration buffer (500 µM $MgCl_2$ and MES buffer containing 200 mM acetosyringone) and 2-3 hours incubation at room temperature performed. For the cell-to-cell movement assay the culture was diluted to an optical density of 0.01–0.001 at 600 nm (OD_{600}). Fully expanded leaves of four-week-old *Nicotiana benthamiana* plants were agroinfiltrated with diluted agrobacterial cultures and the agroinfiltrated plants were maintained under normal growth conditions in a growth room for 3 weeks.

2.6 Cell-to-cell movement assay

To determine whether P3N-PIPO is a necessary factor for cell-to-cell movement of TuMV, transient expression of the PIPO mutant in *Nicotinia benthamiana* leaf cells was used and inoculated leaves were observed under a Leica TCS SP2 inverted confocal microscope with an Argon ion laser in various time intervals. The intervals were 3, 6, and 9 days post inoculation (dpi). Plants tissue inoculated with various PIPO mutants were imaged at room temperature. Distal leaves were examined for systemic infection by GFP localization under UV light and followed by RT-PCR analysis for viral detection after 14 days postinoculation. 5-8 replicates were considered for this assay (Wei et al., 2010).

2.7 Confocal microscopy

For confocal microscopy, YFP was excited at 514 nm and captured at 525-650 nm. CFP was excited at 458 nm and captured at 465–525 nm. GFP was excited at 488 nm and the emitted light was captured at 500 to 555 nm. Images were captured digitally and handled using the Leica LCS software.

2.8 Protoplast isolation and transfection assay

Mesophyll protoplasts were prepared from using leaves from four-week-old *Nicotiana benthamiana* by the Tape-Arabidopsis Sandwich method (Wu et al., 2009). The leaves were incubated in 1–1.5% cellulase Onozuka R-10 and 0.2–0.4% macerozyme R-10 in 0.4 M D-sorbitol, 20 mM KCl and 20 mM MES, pH 5.7 for 2 hours at room temperature. Protoplasts were washed in W5 buffer (154 mM NaCl, 125 mM $CaCl_2$, 5 mM KCl and 2 mM MES, pH 5.7) and resuspended in MMg (0.4 M Mannitol, 15 mM $MgCl_2$, 4 mM MES, PH at 5.7) buffer at a concentration of 10^5 cells/mL. Approximately 5×10^4 protoplasts in 0.2 mL of MMg solution were mixed with approximately 30 (20-40) μg of plasmid DNA at room temperature. An equal volume of a freshly-prepared solution of 40% (w/v) PEG with 0.1 M $CaCl_2$ and 0.2 M mannitol was added, and the mixture was incubated at room temperature for 5 min. After incubation, 3 mL of W5 buffer was added slowly, the solution was mixed, and protoplasts were pelleted by centrifugation at 100 × *g* for 1 min. This protoplast W5 washing step was repeated twice. The protoplasts were resuspended gently in 1 mL of W5 and incubated at room temperature in the light.

Protoplasts were imaged at room temperature after 48 hours post-transfection, using the confocal microscope described above (Vijayapalani et al., 2012).

2.9 RNA extraction and Quantitative reverse transcription –PCR

To verify the level of replication of the introduced mutations *in vivo*, total RNA was extracted from virus-infected TuMV PIPO mutant's protoplasts using the RNeasy Plant Minikit (Qiagen) and treated with RNase-free DNaseI. One microgram of RNA pretreated with DNaseI was used as a template for first strand cDNA synthesis. RT reactions were performed with the SuperScriptIII First-Strand Synthesis System for RT-PCR kit (Invitrogen) according to the manufacturer's instructions. QRT-PCR was performed using SsoFast EvaGreen Supermix (Bio-Rad) in the CFX96 real-time PCR system (Bio-Rad) following the manufacturer's instructions. Relative amounts of all mRNAs were calculated from threshold cycle values. The *Nicotiana benthamiana* actin reference gene was used for normalization. Primers CP-F and CP-R were used for TuMV detection (Wei et al., 2013). Data were statistically evaluated by the unpaired Student's t-test.

2.10 P3N-PIPO artificial frame shift for subcellular localization

Previous high-resolution ultra-structural studies of TuMV revealed that CI protein colocalizes with P3N-PIPO protein and formed conical structures which anchored to and extended through PD (Wei et al., 2010). To investigate whether P3N-PIPO mutants retain their ability for targeting TuMV CI in PD, agrobacterium-mediated transient coexpression was used for subcellular localization studies in this project. A DNA

fragment, which encodes a PIPO-YFP fusion in-frame with the N-terminus of P3 to generate P3N-PIPO-YFP, was constructed. In order to do that, two nucleotides in the G2A6 motif in the TuMV infectious clone was deleted by mutagenic overlap PCR to create an artificial frame shift (Fig. 2.3).

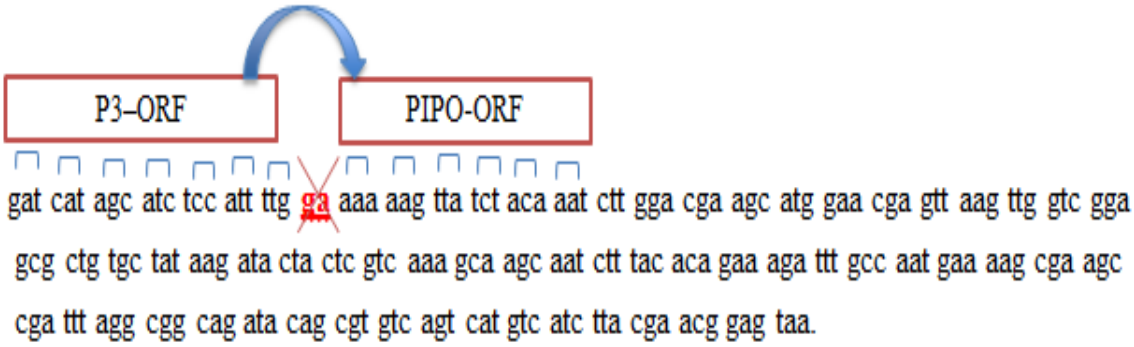

Figure 2.3 Schematic representation of TuMV P3N-PIPO reading frame. The TuMV P3N-PIPO fragment was amplified by artificial frame shift with the introduction of two nucleotides deletion in G2A6 motif of PIPO protein by overlap PCR. The modified fragment was introduced to appropriate destination vectors, which was used for downstream experiments.

2.11 Gateway cloning

Gateway technology (Invitrogen) was used to generate all expression vectors for subcellular localization, bimolecular complementation assay (BIFC) and yeast two hybrid screening (Y2H). Gene sequences were amplified by PCR using Phusion® DNA polymerase (NEB) and primers containing the recombinant sites (Table 2.1). The resulting DNA fragments were separated on 1% agarose gels and then purified using the QIAquick Gel Extraction Kit. The purified fragment was transferred by recombination into the entry vector pDONR221 (Invitrogen) using BP Clonase® enzyme mixtures (Invitrogen) that were set up and incubated overnight at 25 ºC following the supplier's recommendations. Then pDONOR vectors were verified by sequencing (Wei and Wang, 2008). For BIFC and Y2H, the afore-mentioned pDONR221 constructs were ligated with a (35S-YN) gateway or (35S-YC) gateway vector and also a modified (pGADT7) gateway or (pGBKT7) gateway vector respectively (Lu et al., 2010; Xiong and Wang, 2013). For subcellular localization in *Nicotiana benthamiana* plant cells P3N-PIPO mutants and CI modified Gateway fragment ligated with (pEarly101) or (pEarly102) vector to produce P3N-PIPO mutants which were tagged with yellow fluorescence protein (P3N-PIPO-YFP) and CI protein with cyan fluorescent protein (CI-CFP).

Table 2.2 List of primers used for gateway cloning. Gateway sequences were underlined.

Gene ID	Primer Sequence (5′ to 3′)	Target gene
dP3N-PIPO-F	GGGGACAAGTTTGTACAAAAAAGCAGGCTTCATGGGAACAGAATGGGAGGACAC	*P3N-PIPO*
dP3N-PIPO-R	GGGGACCACTTTGTACAAGAAAGCTGGGTCCTCCGTTCGTAAGATGACATG	*P3N-PIPO*
dPIPO-F	GGGGACAAGTTTGTACAAAAAAGCAGGCTTCATGAAAAAGTTATCTACAAATCTTG	*PIPO*
dCI-F	GGGGACAAGTTTGTACAAAAAAGCAGGCTTCATGACTCTCAATGATATAGAGG	*CI*
dCI-R	GGGGACCACTTTGTACAAGAAAGCTGGGTCTTGATGGTGAACTGCCTC	*CI*
PIPO Frame shift-F	TTGAAAAAGTTATCTACAAATCTTGGACGA	*PIPO*
PIPO Frame shift-R	TTTCAAAATGGAGATGCTATGATCCCTC	*PIPO*

2.12 Yeast related methods

2.12.1 Yeast strain and culture

The yeast strain used in this work was the AH109 strain, a derivative of strain PJ69-2A that includes the *ADE2* and *HIS3* markers (James et al., 1996). Yeast cells were grown at 30 °C in either YPD (1% bacto-yeast extract, 2% bacto-peptone and 2% glucose) or in a synthetic dextrose (SD) medium (0.67% bacto-yeast nitrogen base without amino acids, 2% glucose) supplemented with necessary nutrients. To make SD or YPD plates, 2% agar was added to the liquid medium. The SD or YPD media were autoclaved, and stored in 4°C. Yeast cells were stored on SD plates sealed with Parafilm® at 4 °C for up to several months. For long-term storage, yeast cells were grown in an appropriate liquid medium at 30 °C overnight, then 0.6 mL of the culture was added to 0.4 mL of 50% sterile glycerol and stored at -80°C.

2.12.2 Yeast two hybrid screening

Yeast strain AH109 was grown at 28 °C in minimal synthetic defined (SD) base liquid medium [0.17% yeast nitrogen base without amino acids, 2% dextrose] mixed with appropriate drop out (DO) supplement powder. For SD solid medium, SD was supplemented with 1.5% w/v agar. Y2H assays were performed following the Clontech® yeast protocol handbook. In brief, yeast cells were made competent with the LiAC method (Xiong and Wang, 2013) and transformed cells were plated onto a selective medium lacking tryptophan and leucine (SD-Trp-Leu) and a selective medium lacking tryptophan, leucine, histidine, and adenine (SD-Trp-Leu-His-Ade) respectively.

2.13Statistical analysis

All statistical analyses were performed using Microsoft Excel spreadsheet software. Significant differences between the amount of the genomic RNA of mutants relative to that of the wild type virus in the qRT-PCR assay were analyzed using unpaired Student's t-test.

Chapter 3

3 Results

3.1 Knock-out of the P3N-PIPO expression

To test if P3N-PIPO is essential for TuMV cell-to-cell movement, a P3N-PIPO knock-out mutant was created by the introduction of a single stop codon into the PIPO frame without affecting the amino acid sequence of other viral proteins including P3 (Fig. 2.1B). The wild type infectious clone pCambiaTunos/GFP was used as a positive control and the viral replication defective mutant pCambiaTunos/GFP-NIb-GDD (Fellers et al., 1998) was created as a negative control. In the replication-defective mutant, the core motif GDD of the viral RNA-dependent RNA polymerase was mutated to abolish viral replication. The wild type virus, PIPO knock-out and the GDD mutants were agroinfiltrated into *Nicotinia benthamiana* leaf cells. It was found that the PIPO knock-out mutant (GFP-PIPO (R9Stop)) was contained in a single cell only and lost the ability to move to the neighboring cells, even after 9 days post agroinfiltration (dpa) (Fig. 3.1B). In contrast, the leaves agroinfiltrated by the wild type clone (pCambiaTunos/GFP) showed a group of cells of virus infection at 3 dpa that gradually expanded to a large area of virus infection (Fig. 3.1A). As expected, the replication-defective mutant was only found in isolated single cells of *Nicotinia benthamiana* leaves which were agroinfiltrated by the GDD mutant (Fig. 3.1C). The GFP fluorescence derived from the replication-defective GDD mutant came from translation of the non-replicative transcript of the TuMV cDNA (tagged by GFP) under the control of 35S promoter. To monitor if these viruses can establish systemic infection, newly emerging leaves (distal - not infiltrated) were observed under ultraviolet light (UV) for GFP localization after 14 days post

agroinfiltration. Only the wild type clone produced strong green fluorescence signal. This did not occur in other mutants (Fig. 3.2B). Therefore, both PIPO knock-out and GDD mutants cannot move systemically. Consistently, no viral symptoms were evident in plants inoculated with these two mutants 14 dpa (Fig. 3.2B). RT-PCR was conducted to detect the virus in the newly emerging leaves of these plants. No virus was detectable in the new leaves of plants inoculated with these two mutants 14 dpa (Fig. 3.2A).

A) TuMV-GFP

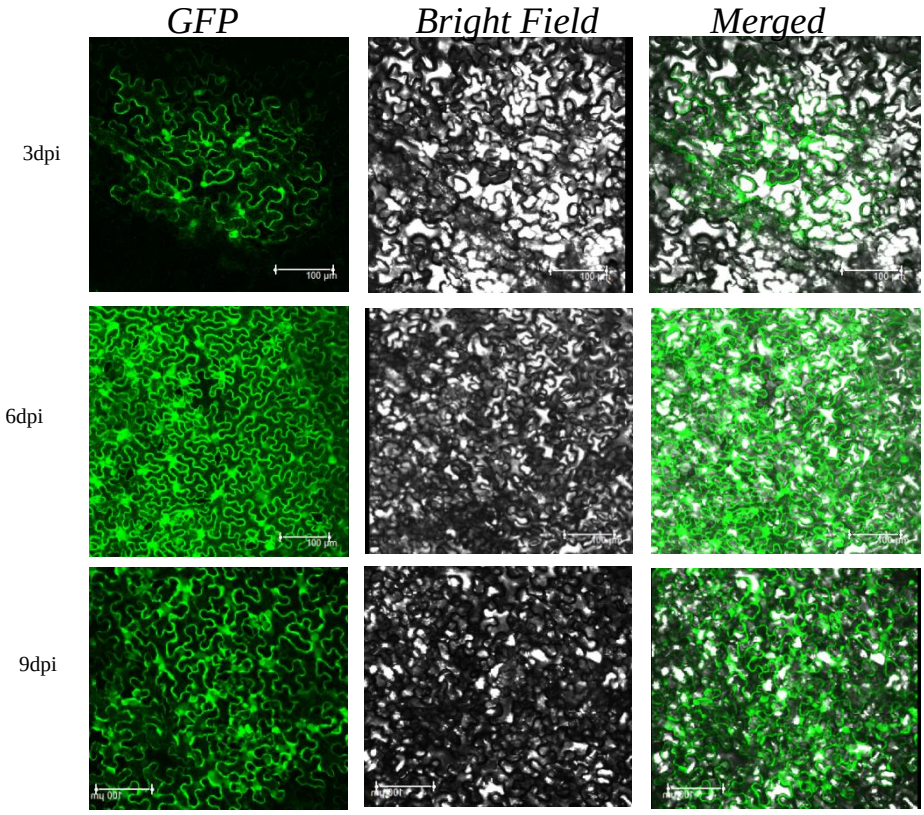

B) GFP-PIPO knock-out

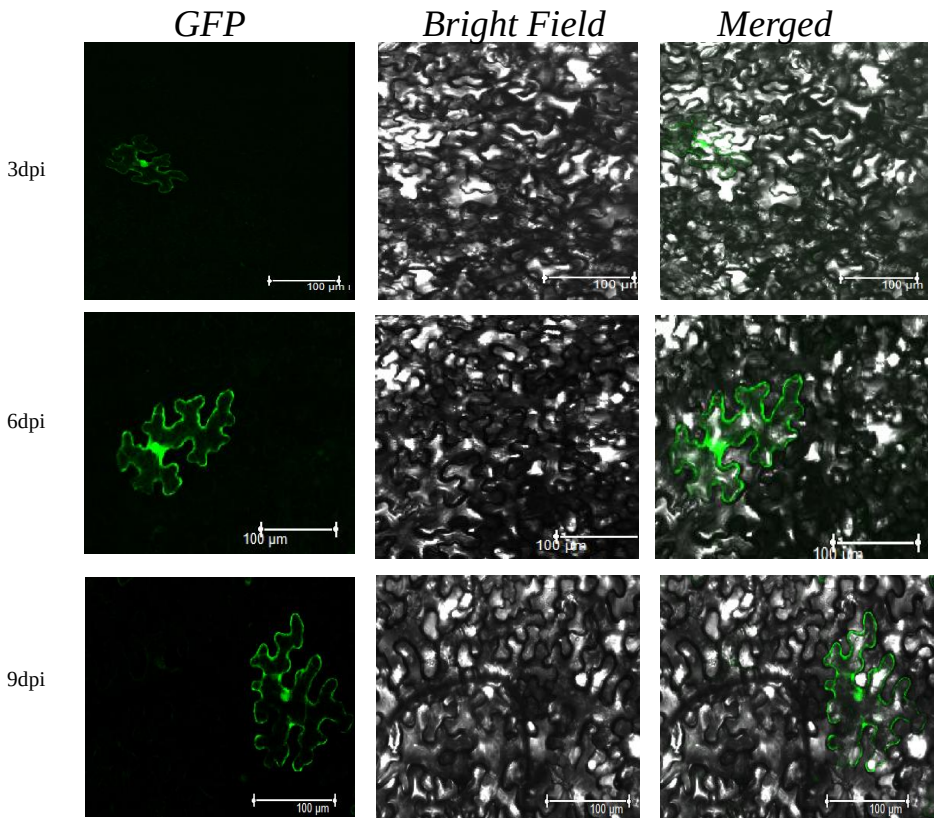

C) GFP/NIb-GDD-TuMV

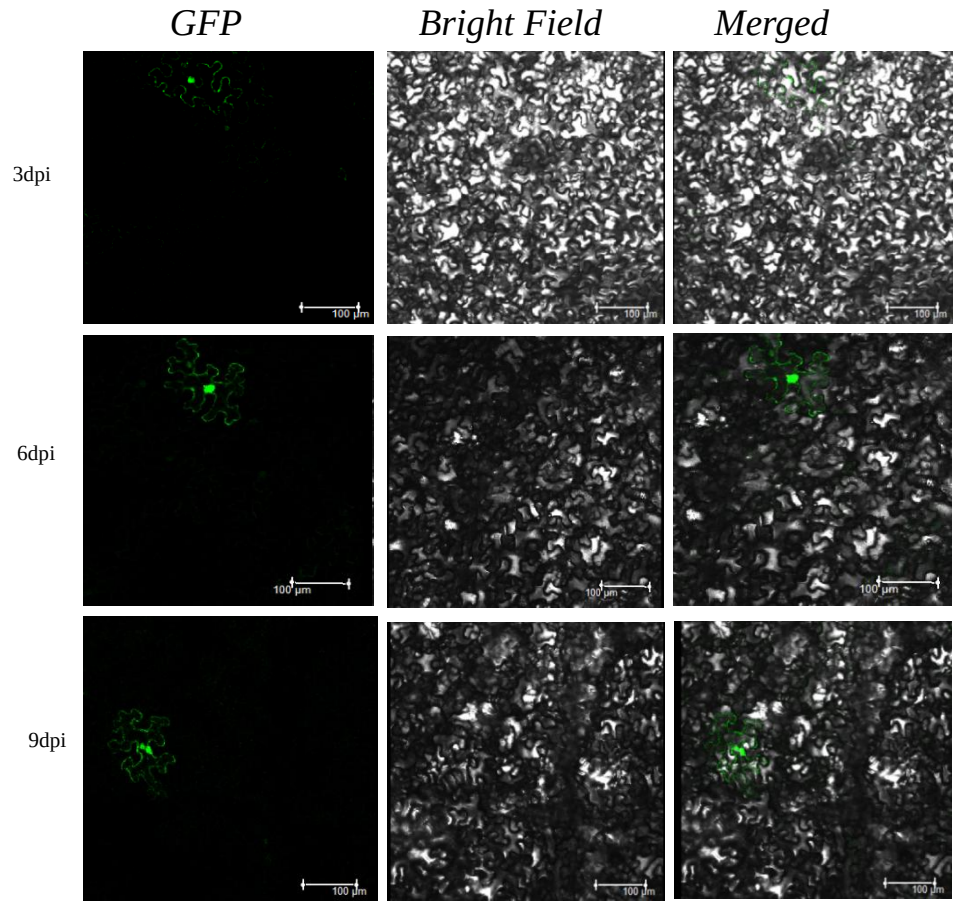

Figure 3.1 Cell-to-cell movement of TuMV requires P3N-PIPO. (A) pCambiaTunos/GFP-TuMV, (B) GFP-PIPO(R9Stop), and (C) GFP/NIb-GDD (negative control) were introduced into *Nicotiana benthamiana* leaves cells via agroinfiltration, respectively. Infiltrated leaves were examined by confocal microscopy 3, 6 and 9 days post infiltration. Scale bar 100 µm.

(A)

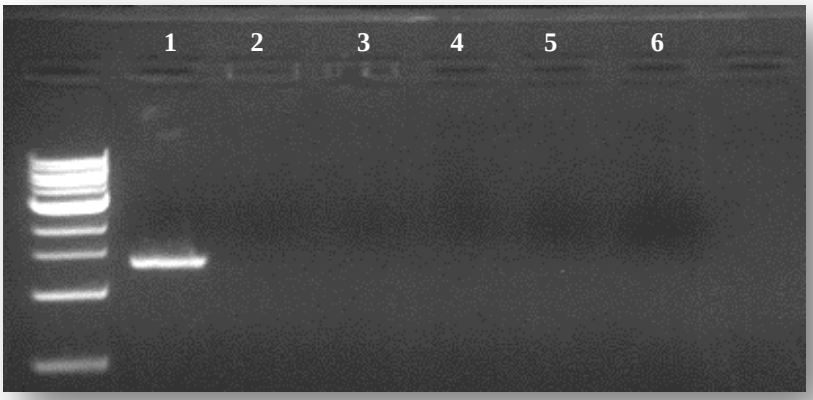

(B)

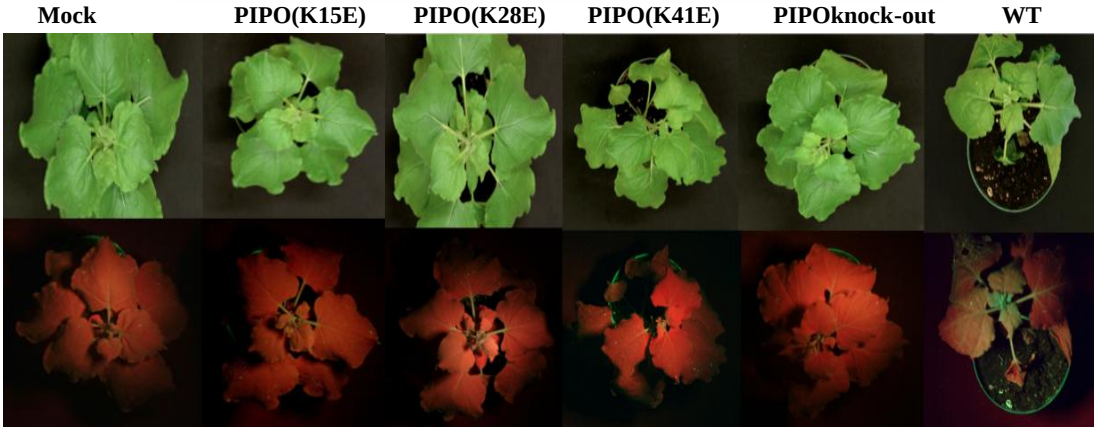

Figure 3.2 Detection of TuMV accumulation in upper newly emerging leaves of *Nicotinana benthamiana* plants inoculated with PIPO mutants. A) Specific TuMV primers were used to amplify a P3N-PIPO cDNA fragment derived from viral RNA isolated from upper newly emerging leaves 14 days post agroinoculation. pCambiaTunos/GFP-TuMV (Lane 1) and TuMV PIPO substitution mutants respectively GFP-PIPO(K15E), GFP-PIPO(K28E), GFP-PIPO(k41E), PIPOknock-out (2, 3, 4 and 5) and mock (Lane 6). B) *Nicotinia benthamiana* leaves were infected with pCambiaTunos/GFP-TuMV and TuMV PIPO mutants 14 days post inoculation under normal and UV light.

3.2 Synonymous mutations in P3N-PIPO

The substitution mutation in PIPO also was performed by site-directed mutagenesis. These mutations were synonymous with respect to the polyprotein frame. They resulted in replacement of a negatively charged amino acid with positively charged residue. A total of three mutants were derived through these substitutions: PIPO(K15E), PIPO(K28E), and PIPO(K41E) (Fig. 3.3). Transient expression of PIPO mutants in *Nicotinia benthamiana* leaf cells was subsequently performed and agroinfiltrated leaves cells were observed by confocal microscopy in different time intervals (3, 6, and 9 days post agroinfiltration) (Fig. 3.3). Moreover, RT-PCR results of newly emerging leaves (not inoculated ones) and GFP localization assay under UV light showed the same GFP fluorescence pattern as the knock-out mutant and no indication of viral symptoms was determined 14 day post agroinfiltration (Fig. 3.2 A and B).

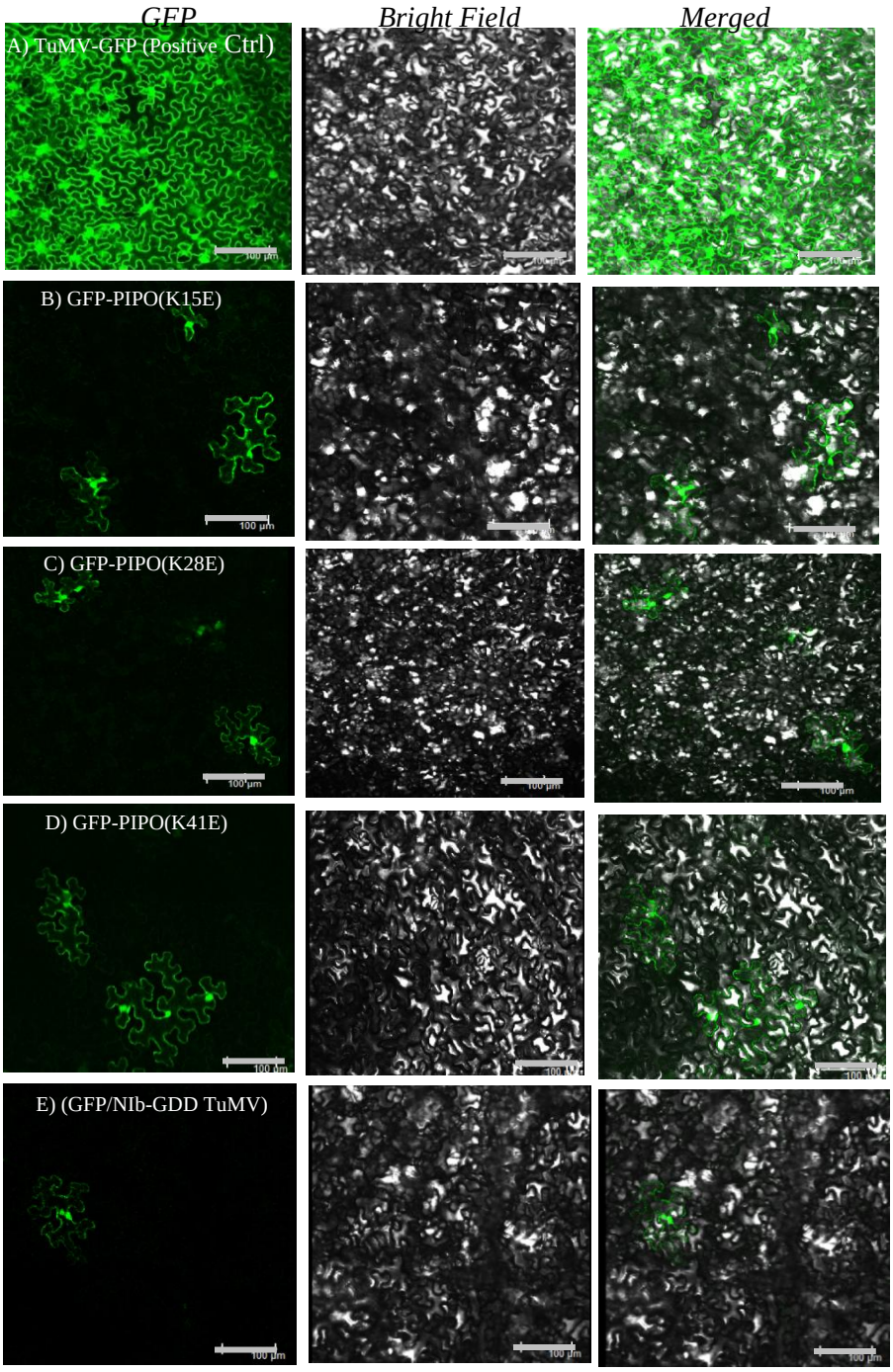

Figure 3.3 TuMV P3N-PIPO substitution mutants impaired intercellular movement. (A) pCambiaTunos/GFP-TuMV, (B) GFP-PIPO(K15E), (C) GFP-PIPO(K28E), (D) GFP-PIPO(K41E), and (E) GFP-NIb-GDD-TuMV(negative control) were introduced into *Nicotiana benthamiana* via agroinfiltration, respectively. Images were taken 9 days post inoculation. Scale bar 100 µm.

3.3 Protoplast transfection and quantitative RT-PCR assay

Since three PIPO substitutions mutants [PIPO(K15E), PIPO(K28E), PIPO(K41E)] and PIPO knock-out mutant lost ability to move between cells, it is necessary to determine if these mutations affect viral replication (Fig. 3.4). The wild type virus and all the five mutants including three substitution mutants, PIPO knock-out mutant and the replication-defective GDD mutant were subjected to the replication assay in protoplasts. The strong green fluorescence signal, similar to the wild type, was observed of transfected protoplast by PIPO mutants. Weak GFP signals were also evident for the GDD mutant due to transcription of the viral cDNA directed by the constitutive 35S promoter. Quantitative RT-PCR was applied to compare the TuMV transcript levels of different PIPO mutants in protoplast. For this purpose, total RNA was extracted from transfected protoplast 22 hours post transfection and followed by real time PCR with specific TuMV primers. The result showed that knock-out or substitution mutations of P3N-PIPO did not significantly affect TuMV viral replication (Fig. 3.5).

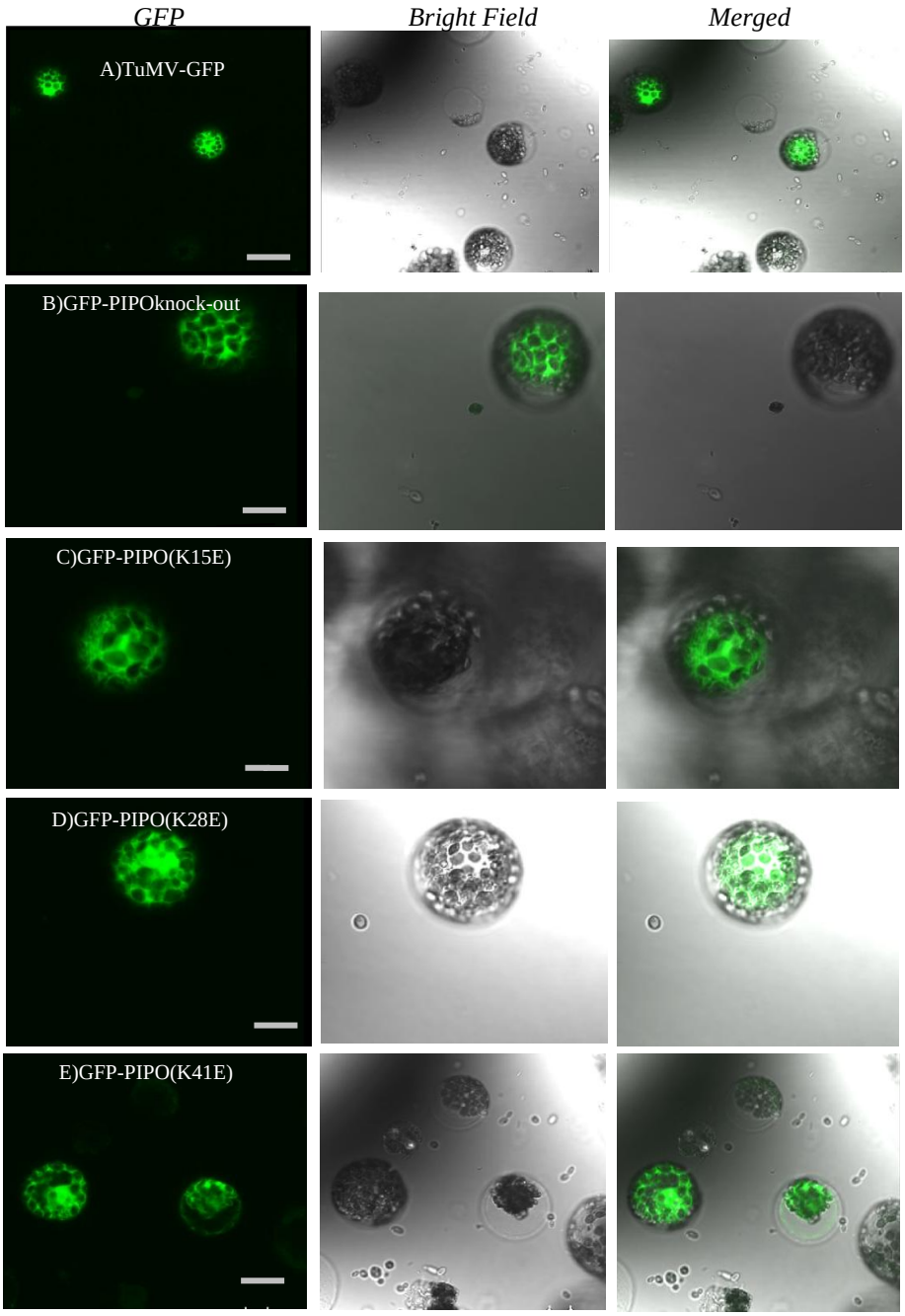

Figure 3.4 Replicaiton assay of TuMV P3NPIPO mutants in *Nicotiana benthamiana* mesophyll protoplasts. (A) pCambiaTunos/GFP-TuMV, (B) PIPO knock-out, (C) GFP-PIPO(K15E), (D) GFP-PIPO(K28E), (E) GFP-PIPO(K41E) were transfetcted into the isolated protoplasts, respectively. Images were taken 48 hours after transfection. Scale bar 10 μm.

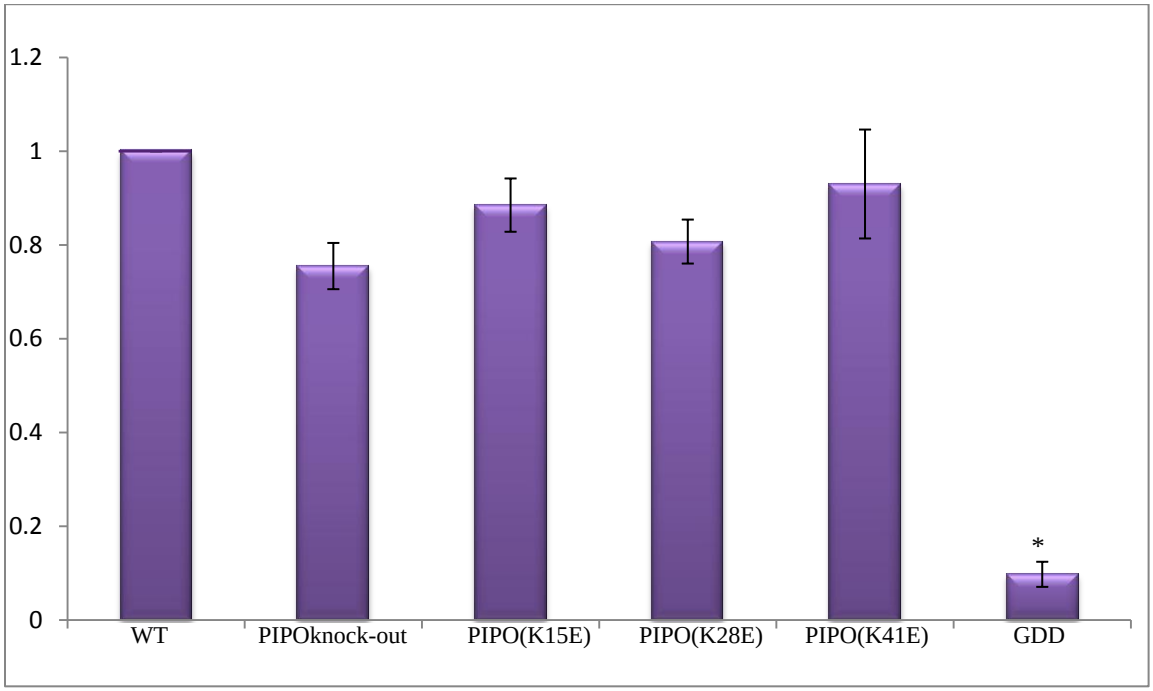

Figure 3.5 RT-PCR quantification of PIPO mutants RNA in protoplast. RNA was extracted from transfected protoplast after 22 hours. The TuMV RNA levels were normalized to the amount of actin transcript in each sample and then further to that of wild type virus (pCambiaTunos/GFP-TuMV (WT). The values SEs were calculated from three biological replicates. Statistical significance was analyzed by the unpaired Students t-test and ($P<0.05$)*.

3.4 P3N-PIPO mutants lost their ability to target the TuMV CI protein

To examine why P3N-PIPO mutations affect cell-to-cell movement, I determined the subcellular localization of TuMV P3N-PIPO and further tested if TuMV P3N-PIPO mutants still have ability to direct the targeting of CI to PD. Consistent with the distribution of TEV P3N-PIPO, TuMV P3N-PIPO-YFP was also located at PD in *Nicotiana benthamiana* epidermal cells (Fig. 3.6 B). When expressed alone, the TuMV CI protein formed aggregates in the cytoplasm (Fig. 3.6 A). However, when TuMV CI and P3N-PIPO were coexpressed, both of them targeted the PD (Fig. 3.7A). This is in agreement with the previous finding that TEV P3N-PIPO modulates the PD-localization of TEV CI (Wei et al. 2010). However, coexpression of the TuMV PIPO knock-out mutant (which is P3N, N-terminal portion of P3) and TuMV CI failed to direct CI to PD and both proteins were present in the cytoplasm as aggregates (Fig. 3.7 B). These data suggest that PIPO is essential for PD-localization of P3N-PIPO and for directing CI to PD. Coexpression of TuMV CI with P3N-PIPO substitution mutants revealed that these P3N-PIPO mutants lost the ability to target the CI protein to PD (Fig. 3.8 A, B and C). To examine if these P3N-PIPO mutants remain to be PD-located proteins like P3N-PIPO, they were coexpressed with the PD marker PDLP1 (PD-located protein 1). The results showed that the P3N-PIPO mutants still maintained their ability for PD localization (Fig. 3.9).

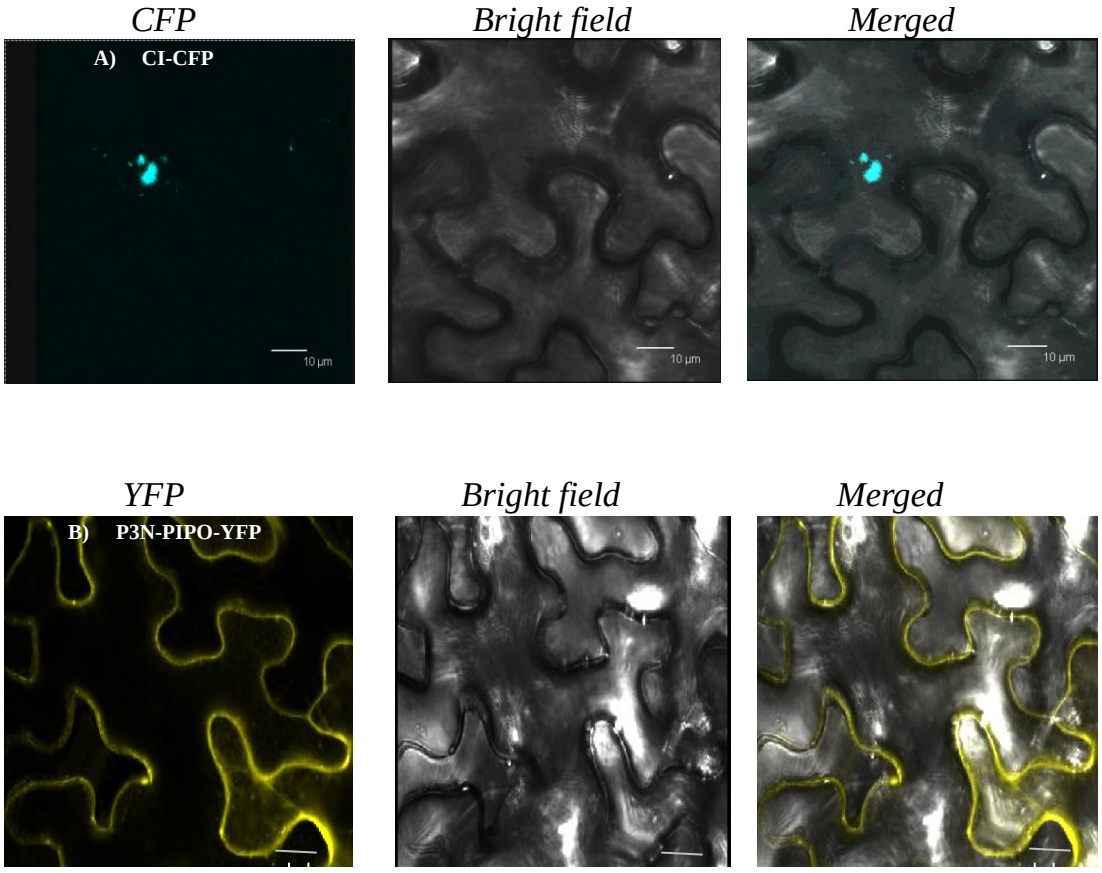

Figure 3.6 Subcellular localization of TuMV CI and P3N-PIPO proteins in *Nicotiana benthamiana* leaf cells. Transient expression of CI-CFP (A) and P3N-PIPO-YFP (B) was examined by confocal microscopy. Images were taken 48 hrs post agroinfiltration. Scale bar 10 µm.

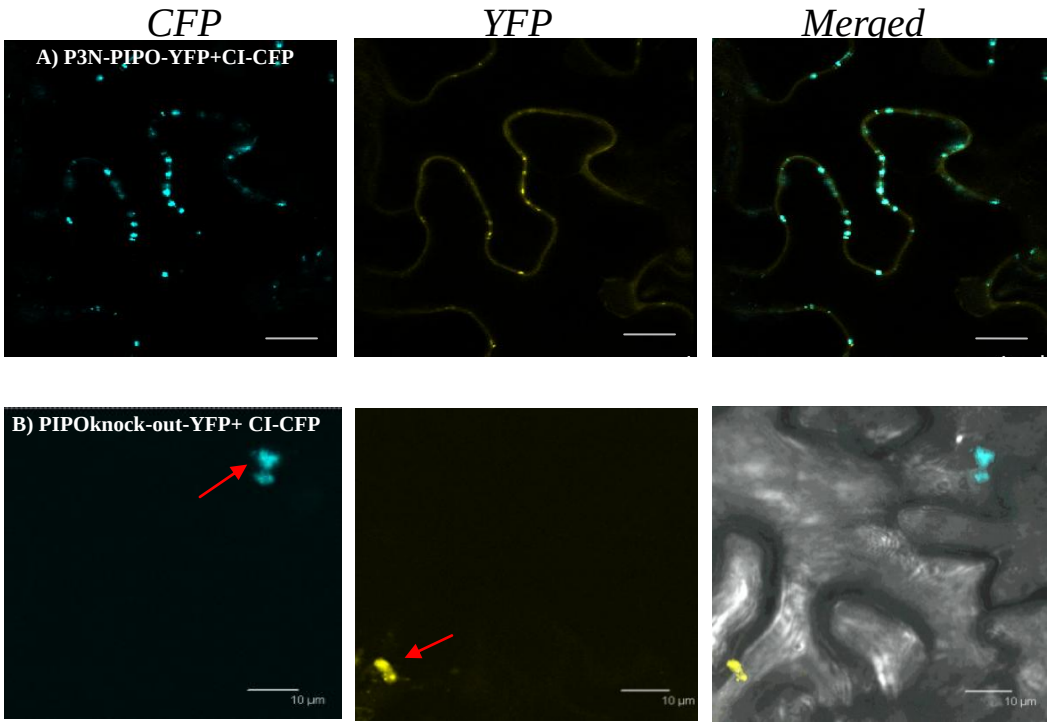

Figure 3.7 Subcellular localization of TuMV CI in *Nicotiana benthamiana* leaf cells. Transient coexpression of CI-CFP with P3N-PIPO-YFP (wild type) (A) or with the PIPO knock-out mutant (B) was examined by confocal microscopy. Images were taken 48 hrs post agroinfiltration. The arrows indicated the aggregates of both proteins in cytoplasm. Scale bar 10 µm.

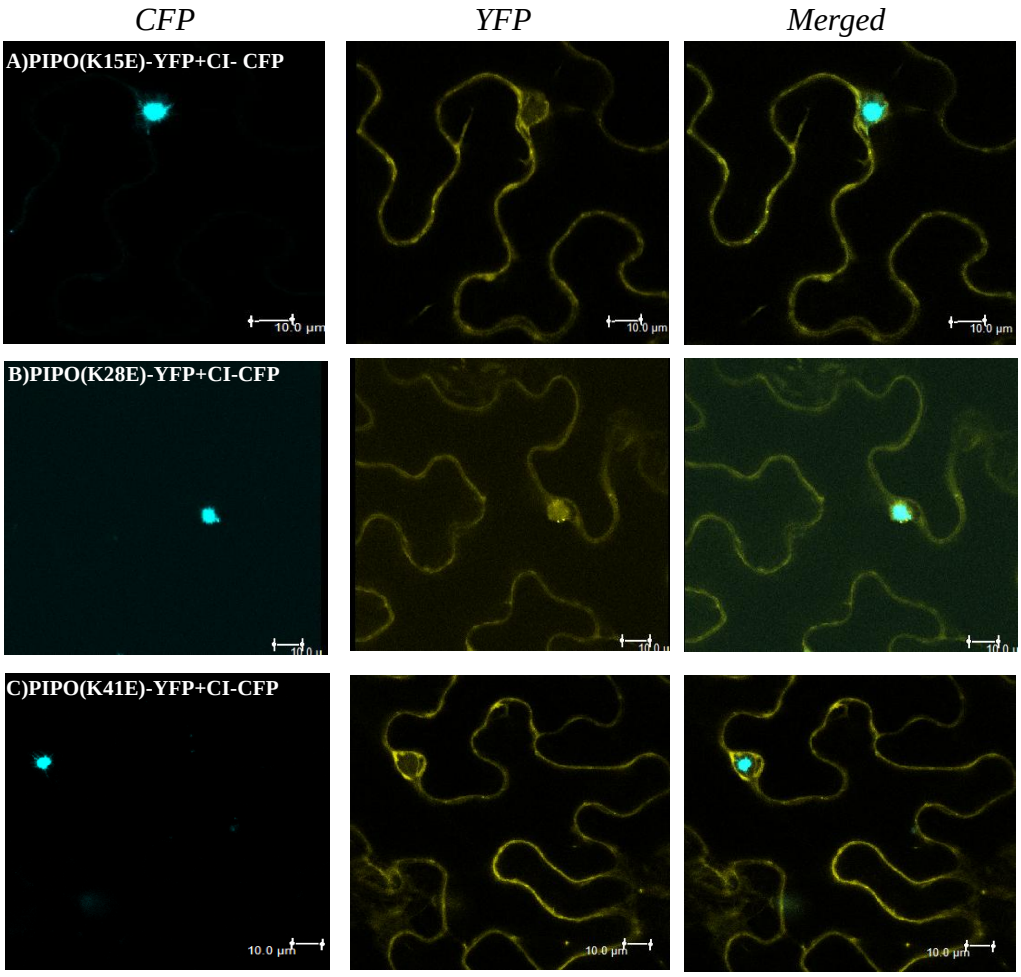

Figure 3.8 Subcellular localization substitutions of PIPO mutants in *Nicotiana benthamiana* leaf cells. Transient coexpression of CI-CFP with the PIPO(k15E)-YFP (A), PIPO(K28E)-YFP (B), PIPO(K41E)-YFP (C) was observed under a confocal microscope. Images were taken 48 hrs post agroinfiltration. Scale bar 10 µm.

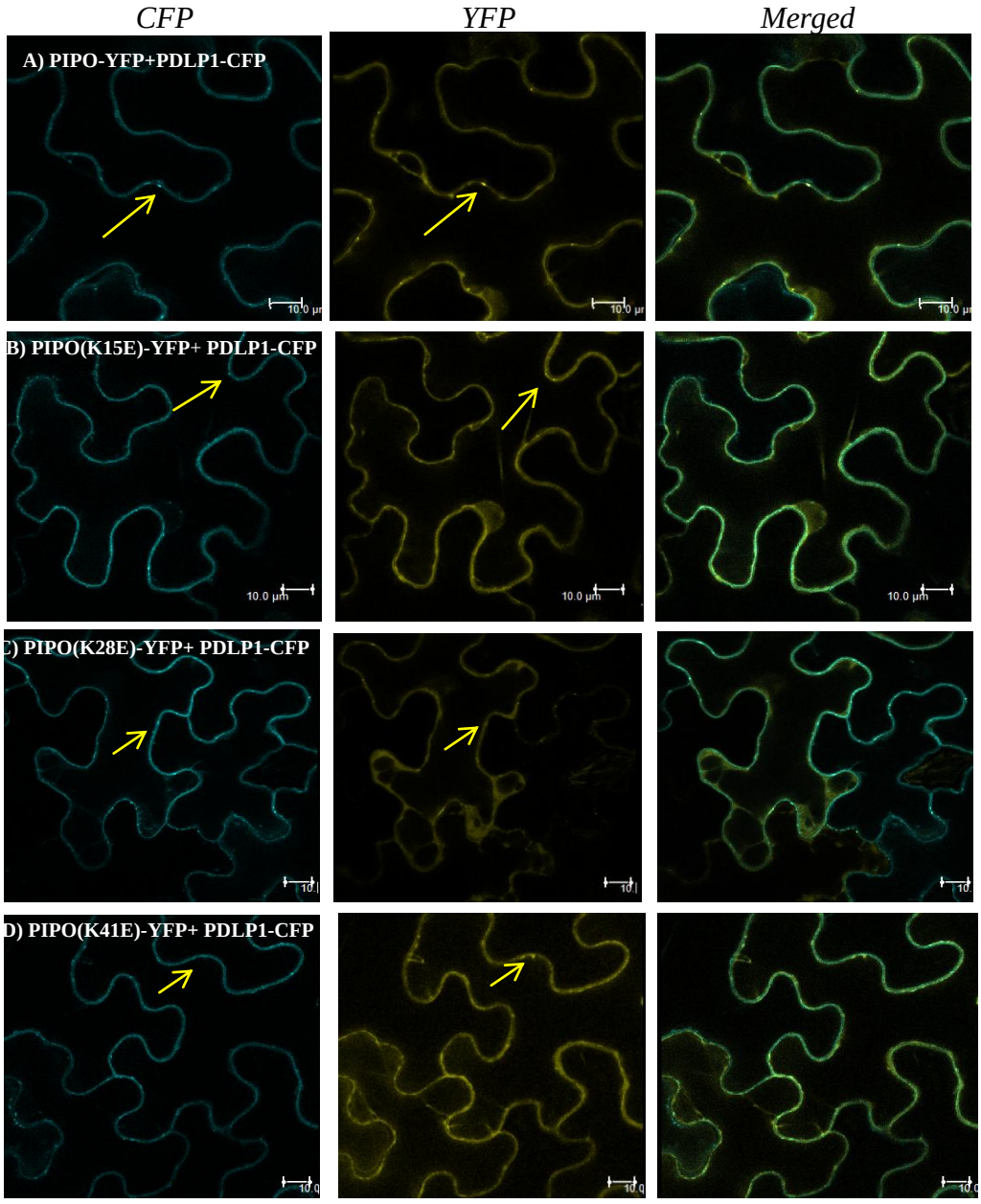

Figure 3.9 P3N-PIPO substitution mutants keep their ability for PD localization in *Nicotiana benthamiana* leaf cells. Transient coexpression of PDLP-CFP (PD marker) with P3NPIPO-YFP wild type (A), PIPO(K15E)-YFP (B), PIPO(K28E)-YFP (C), and PIPO(K41E)-YFP (D) was monitored by confocal microscopy. Images were taken 48 hrs post agroinfiltration. The arrows indicated the colocalization of two proteins. Scale bar 10 µm.

3.5 The P3N-PIPO mutants lost the ability for interaction with TuMV CI in PD

To assess the possibility of interactions of P3N-PIPO mutants and CI protein *in planta*, then bimolecular fluorescence complementation (BIFC) assay was carried out and leaf epidermal cells were observed under the confocal microscope after 48 hours post agroinfiltration. P3N-PIPO mutants and CI protein were translationally fused at the N- (YN) and the C-terminal half (YC) of YFP, respectively or in the reciprocal combination (Appendix. A). P3NPIPO-YC mutants and CI-YN were transiently coexpressed in *Nicotinia benthamiana* plants by agroinfiltration. A strong yellow fluorescence was observed in PD of cells coexpressing P3N-PIPO-YC and CI-YN (Fig. 3.10 B). However, yellow fluorescence signal was not observed in infiltrated *Nicotinia benthamiana* leaf cells coexpressing P3N-PIPO-YC mutants with CI-YN (Fig. 3.10). The P3N-PIPO mutants which had defective cell-to-cell movement were examined for interactions with TuMV CI protein in yeast two-hybrid systems (Y2H). Co-transformants were selected and plated on selective media to detect activation of the reporter genes *ADE2* and *HIS3*. No positive reaction was observed either between P3N-PIPO (wild type one) and CI protein or between P3N-PIPO mutants and CI on selective media (Fig. 3.11) or in the reciprocal combination (Appendix. B).

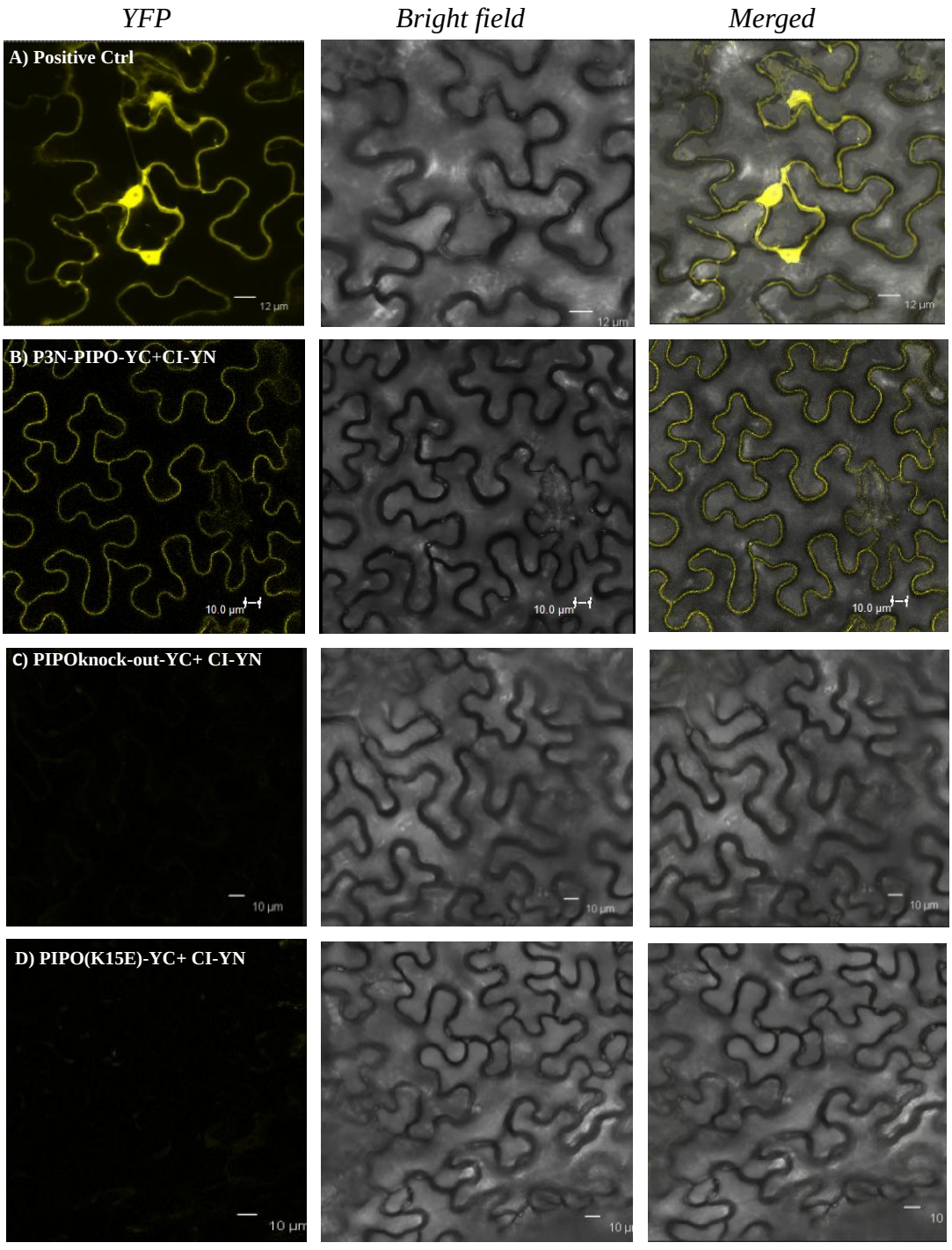
YFP
Bright field
Merged
A) Positive Ctrl
B) P3N-PIPO-YC+CI-YN
C) PIPOknock-out-YC+ CI-YN
D) PIPO(K15E)-YC+ CI-YN

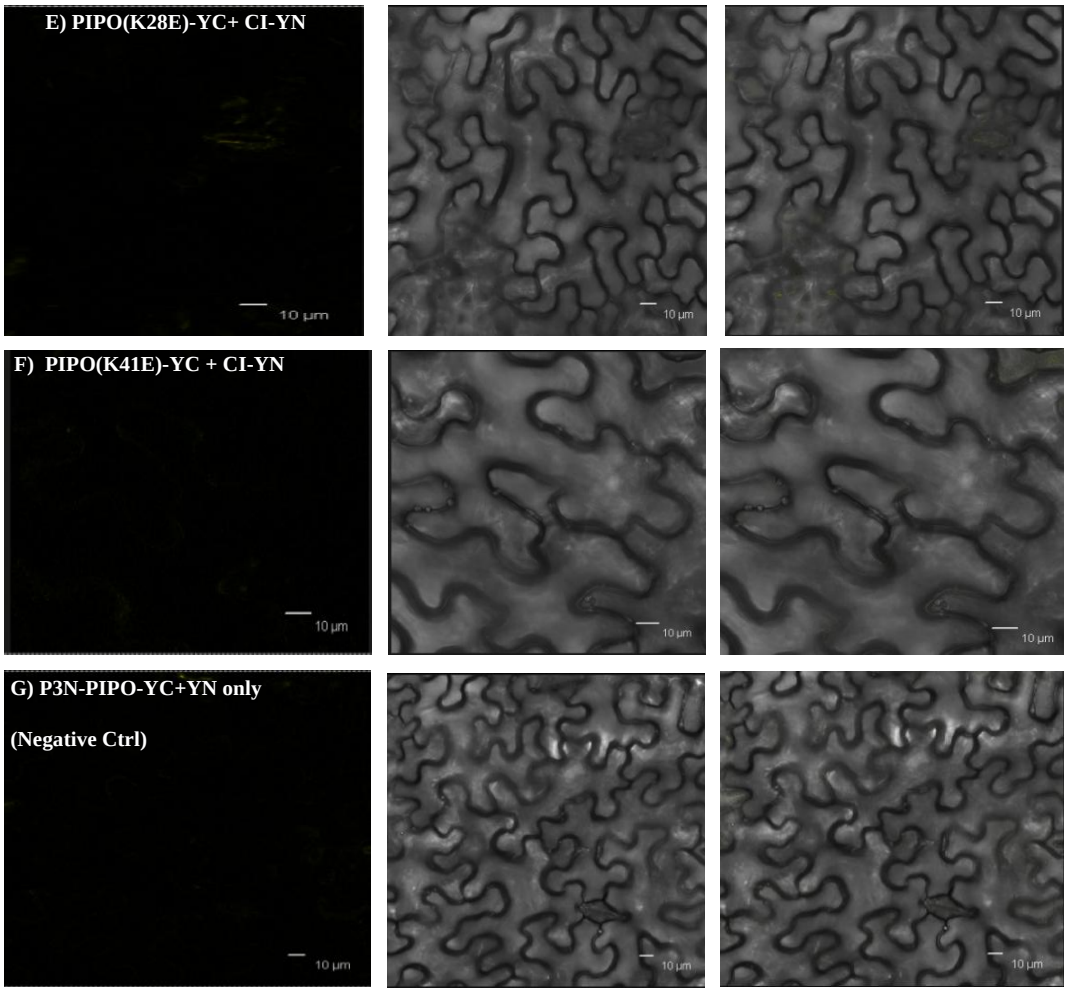

Figure 3.10 TuMV PIPO mutants lose their ability for interaction with CI protein in planta. Bimolecular fluorescence complementation (BIFC) of P3N-PIPO knock-out, substitution mutants and TuMV CI protein in *Nicotiana benthamiana* plants. Extended leaves of three-week-old seedlings were coagroinfiltrated with TuMV CI-YN and CI-YC (positive control) (A), P3N-PIPO-YC mutants and CI-YN (C through F), and P3N-PIPO-YC and YN only (negative control). Yellow fluorescence signals were monitored two days after agroinfiltration, using a confocal microscope. Scale bar 10 µm.

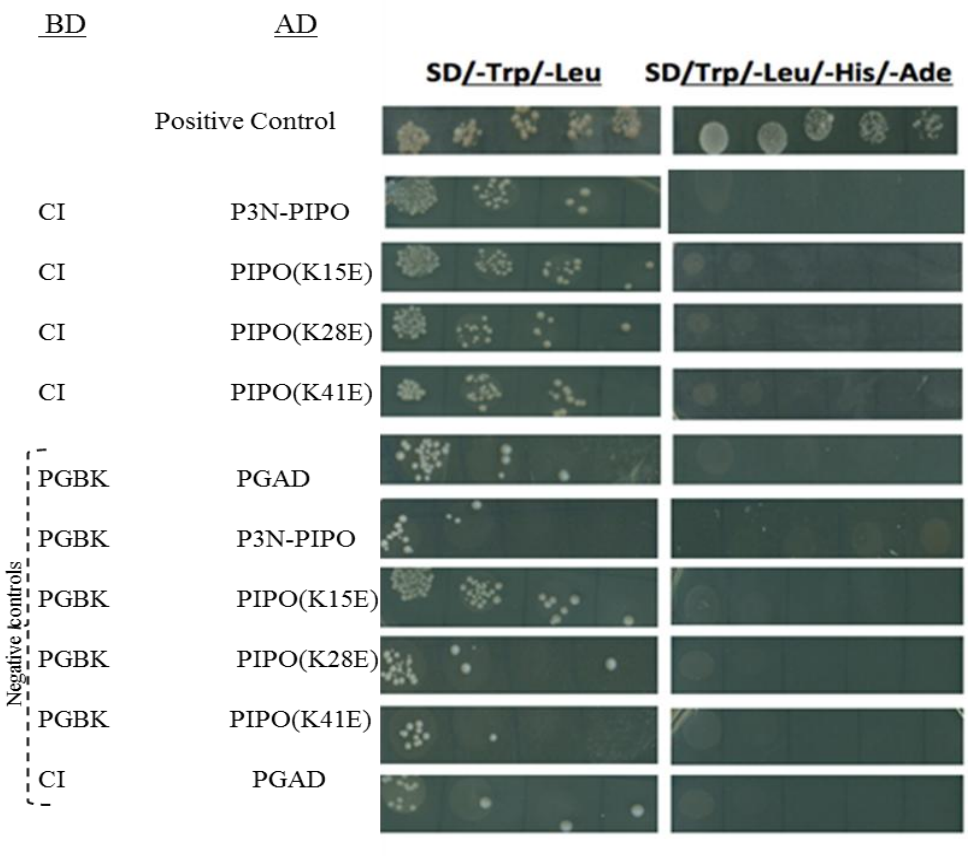

Figure 3.11 P3N-PIPO or P3N-PIPO mutants do not interact with TuMV CI protein in the yeast two-hybrid assay. Yeast two-hybrid assay of protein-protein interaction between P3N-PIPO and CI, or between P3N-PIPO mutants PIPO(K15E), PIPO(K28E), PIPO(K41E) and TuMV CI protein. Ten-fold serial dilutions of cultures of yeast co-transformants were grown on the selective medium.

3.6 P3N-PIPO and CI interactions in plant cells co-localized with CI protein and formed a thread like structure

The mixture of agarobacterial culture composed of BIFC complex (P3N-PIPO-YC, CI-YN) and CI-CFP plasmids coagroinfiltrated in 2:1 ratio manner in *Nicotiana benthamiana* leaf cells. The yellow fluorescent signals from the P3N-PIPO and CI interactions (the BIFC complex) colocalized with the CI-CFP fusion protein after 48 hours post agroinfiltration (Fig. 3.12A). Under higher magnification, it is evident that the cyan fluorescence of CI-CFP fusion protein extended inwards from the PD-located CI-P3N-PIPO interaction site and also penetrated though PD to reach the neighboring cell (Fig. 3.12). The data suggested that the P3N-PIPO protein anchors the CI protein at PD via its interaction with CI and the further extension of the CI structure may be through the CI-CI self-interaction.

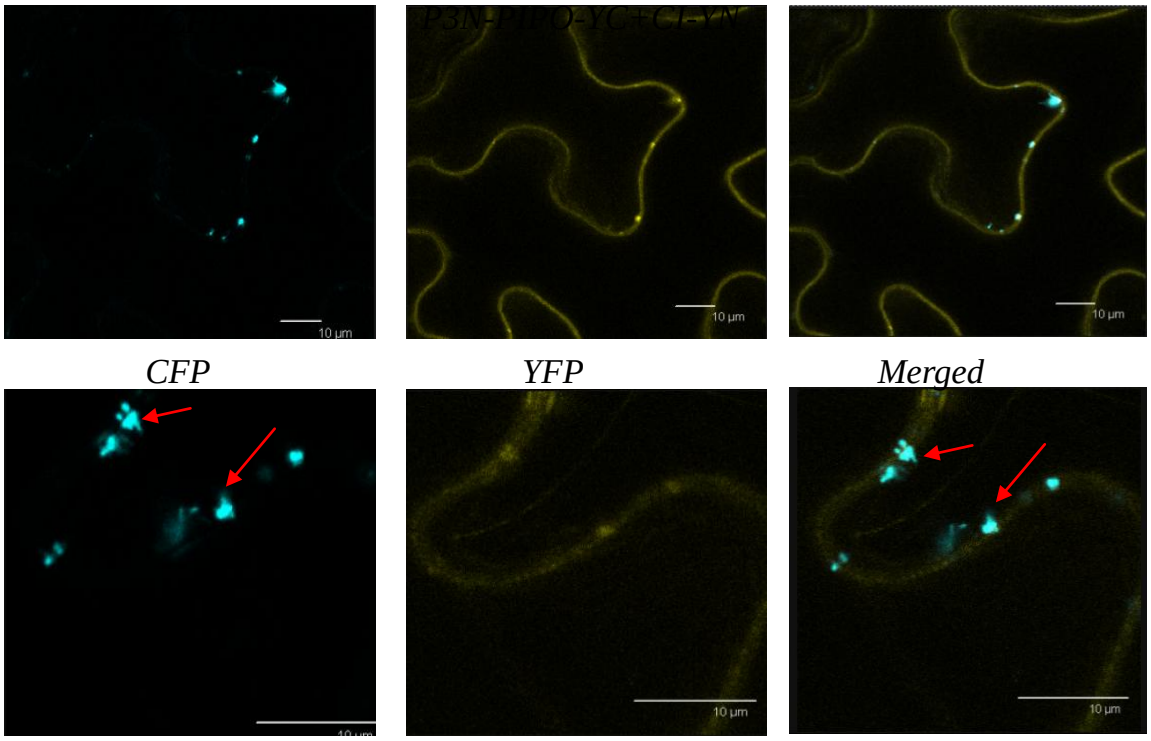

Figure 3.12 Colocalization of BIFC complex (P3N-PIPO-YC :: CI-YN) and TuMV CI-CFP protein in planta. Infiltrated *Nicotiana benthamiana* leaves cells were observed under a confocal microscope. Images in top panels were taken 48 hrs post agroinfiltration and images in low panels 72 hrs post agroinfiltration. The arrow points to the CI structure extended inwards from PD. Scale bar 10 µm.

3.7 The N-terminal portion of TuMV CI protein is responsible for P3N-PIPO interaction

To test which fragment(s) of CI are responsible for interactions with P3N-PIPO, expression vectors for the transient expression of the N- and C-terminal fragments of CI were constructed based on their predicted conserved domain structure (Fig. 3.13). BIFC analysis in *Nicothinia benthaminia* leaves cells and Y2H assay in yeast revealed that the positive interaction of the N-terminal half of the CI protein (1-334 aa) containing the most conserved motifs for helicase activity with TuMV P3N-PIPO (Fig. 3. 15and 3.16). No positive interaction with PN3-PIPO was detected for the C-terminal region of CI (335-644aa) (Fig. 3.15 and 3.16). The data indicated that the N-terminal region of TuMV CI protein is responsible for the P3N-PIPO interaction. To further map the region responsible for the interaction with P3N-PIPO, the N-terminal half of CI protein (1-334 aa) was split into two fragments CIF3 (1-213aa) and CIF4 (214-334aa) (Fig. 3.16). The BIFC results were positive for both the N-terminal portions (CIF3, CIF4) with P3N-PIPO *in planta*. However, the distribution patterns of their interacting complexes were different (Fig. 3.17). CIF3 interacted with P3N-PIPO took place in PD, whereas the interacting complex of CIF4 and P3N-PIPOs was found apparently in the cytoplasm and nucleus (Fig. 3.17 A and B). Interestingly, Y2H assay identified only the CIF3 and P3N-PIPO interaction but not for the CIF4 and P3N-PIPO interaction (Fig. 3.18).

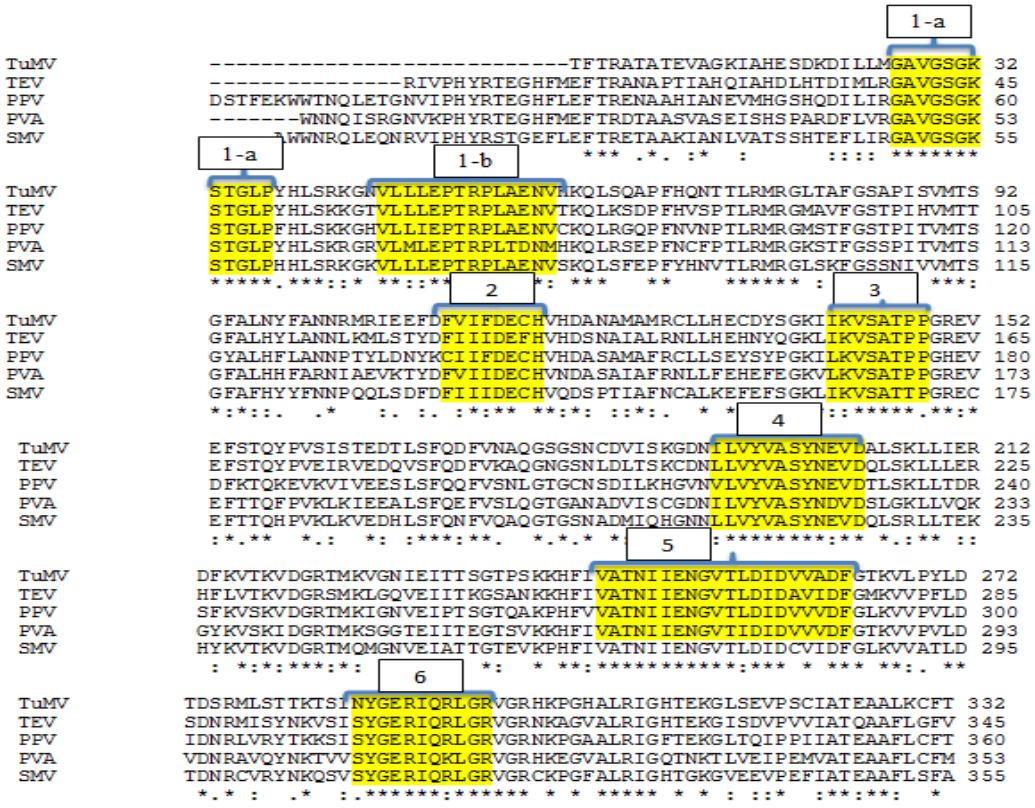

Figure 3.13 Multi-sequence alignments of the CI proteins of potyviruses TuMV, TEV, PPV, PVA and SMV. The alignment was done using the CLUSTAL W program: TuMV (GenBank accession no. NC002509), PPV (*Plum pox virus*; GenBank accession no. P13529), PVA (*Potato A virus*; GenBank accession no. Q85197), PVY (*Potato Y virus*; GenBank accession no. S70722), SMV (*Soybean mosaic virus*; GenBank accession no. Q90069), and TEV (*Tobacco etch virus*; GenBank accession no. P04517). Ordinal numbers indicated conserved motifs in CI proteins.

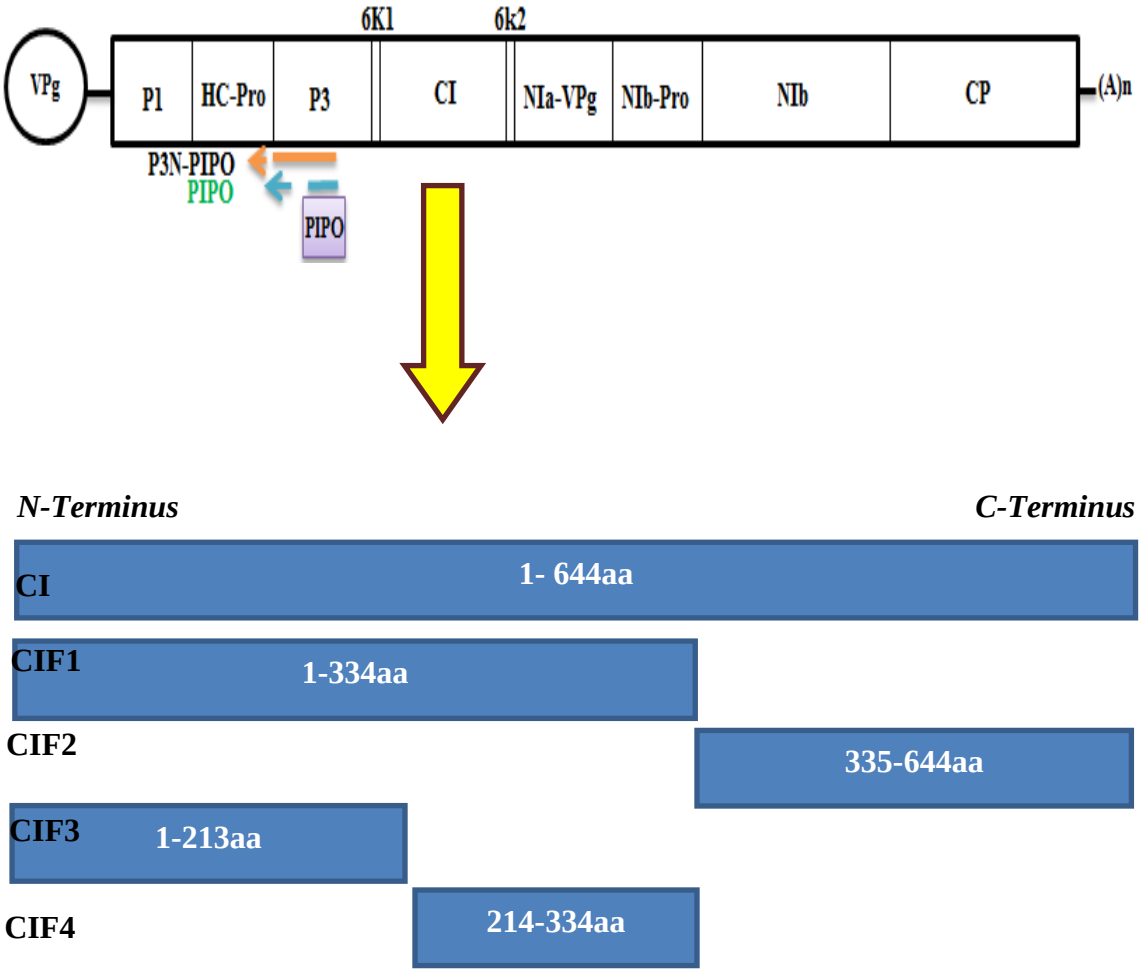

Figure 3.14 Schematic representation of full length of TuMV CI protein. CIF1, CIF2, CIF3, CIF4 represent desired fragments, which were studied independently in terms of interaction with TuMV P3N-PIPO.

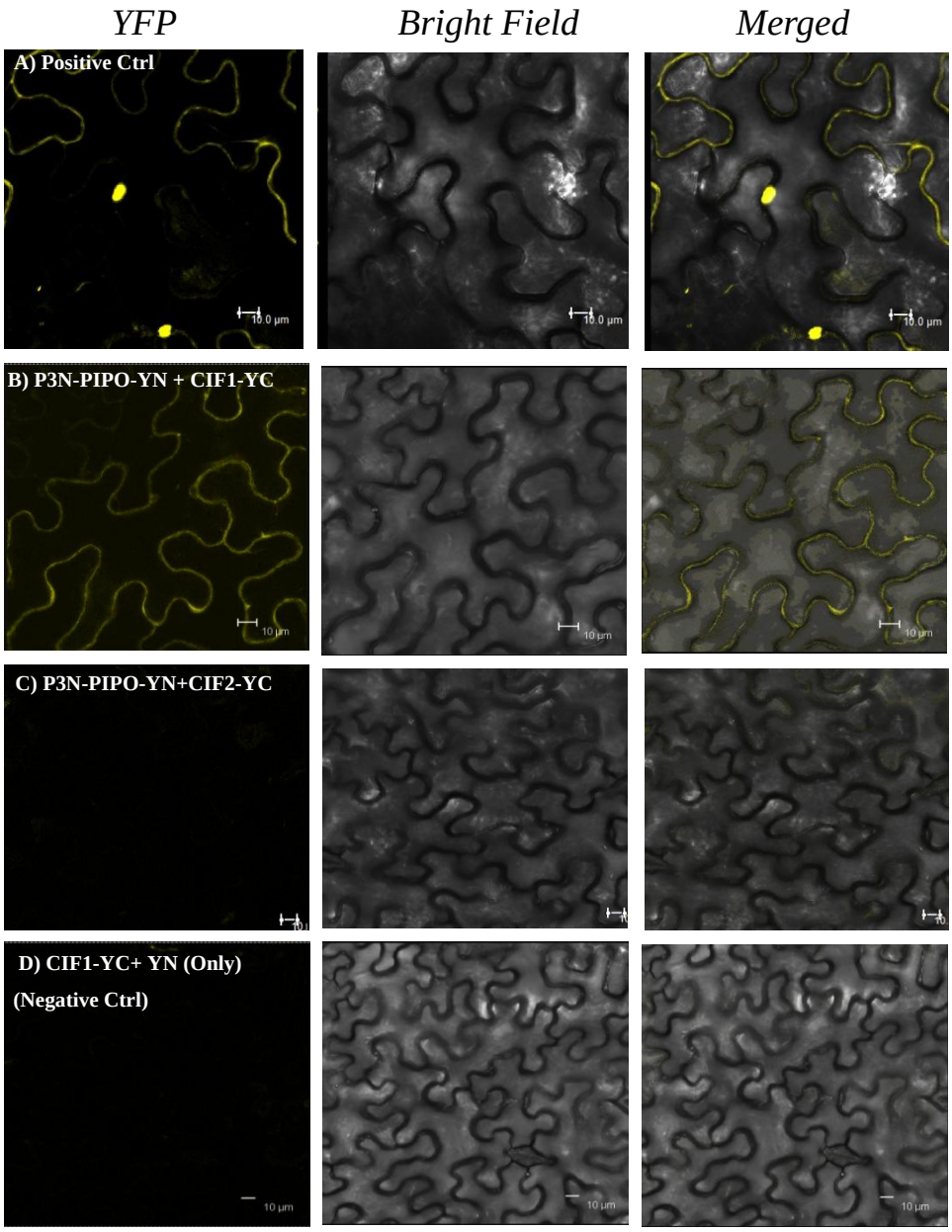

Figure 3.15 The N-terminal region of TuMV CI interacts with P3NPIPO *in planta*. BIFC interaction assay for P3N-PIPO and CIF1 (1-334 a.a), CIF2 (335-644 a.a). *Nicotiana benthamiana* leaves were observed under a confocal microscope after two days post agroinfiltration. Scale bar 10 µm.

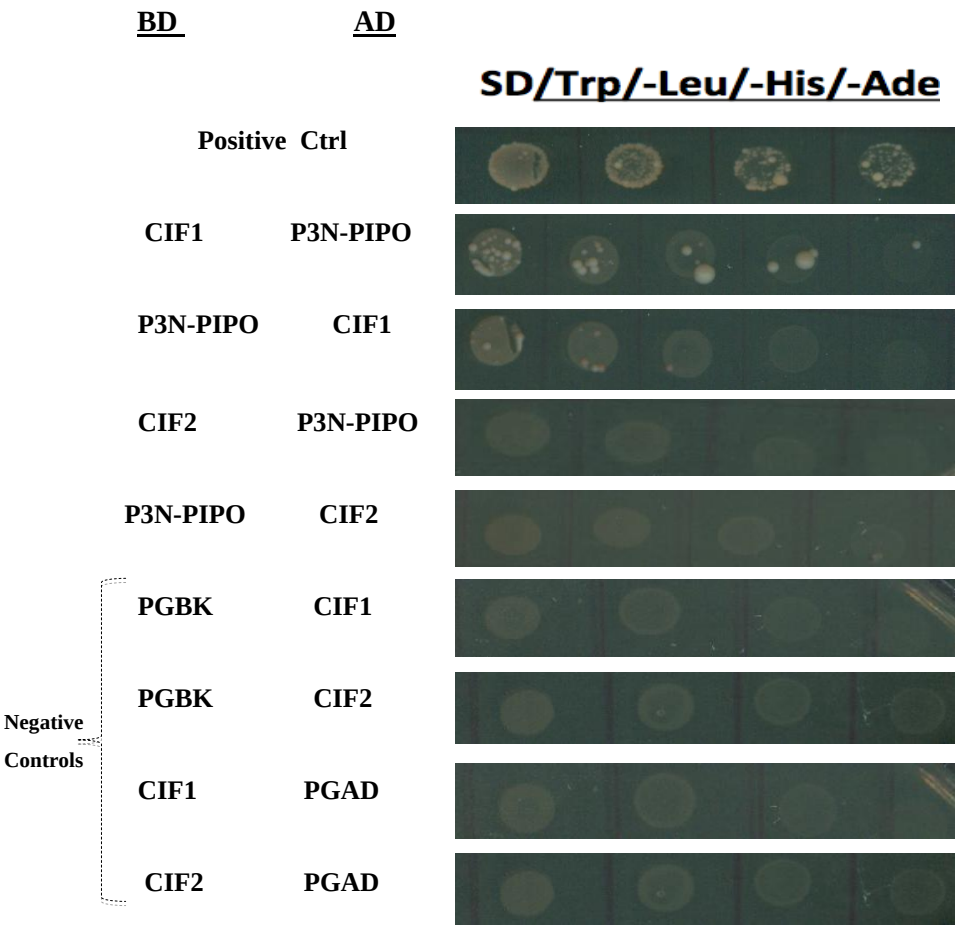

Figure 3.16 The N-terminal region of TuMV CI interacts with P3N-PIPO in the yeast two-hybrid assay. Ten-fold serial dilutions of cultures of yeast co-transformants were grown on the selective medium.

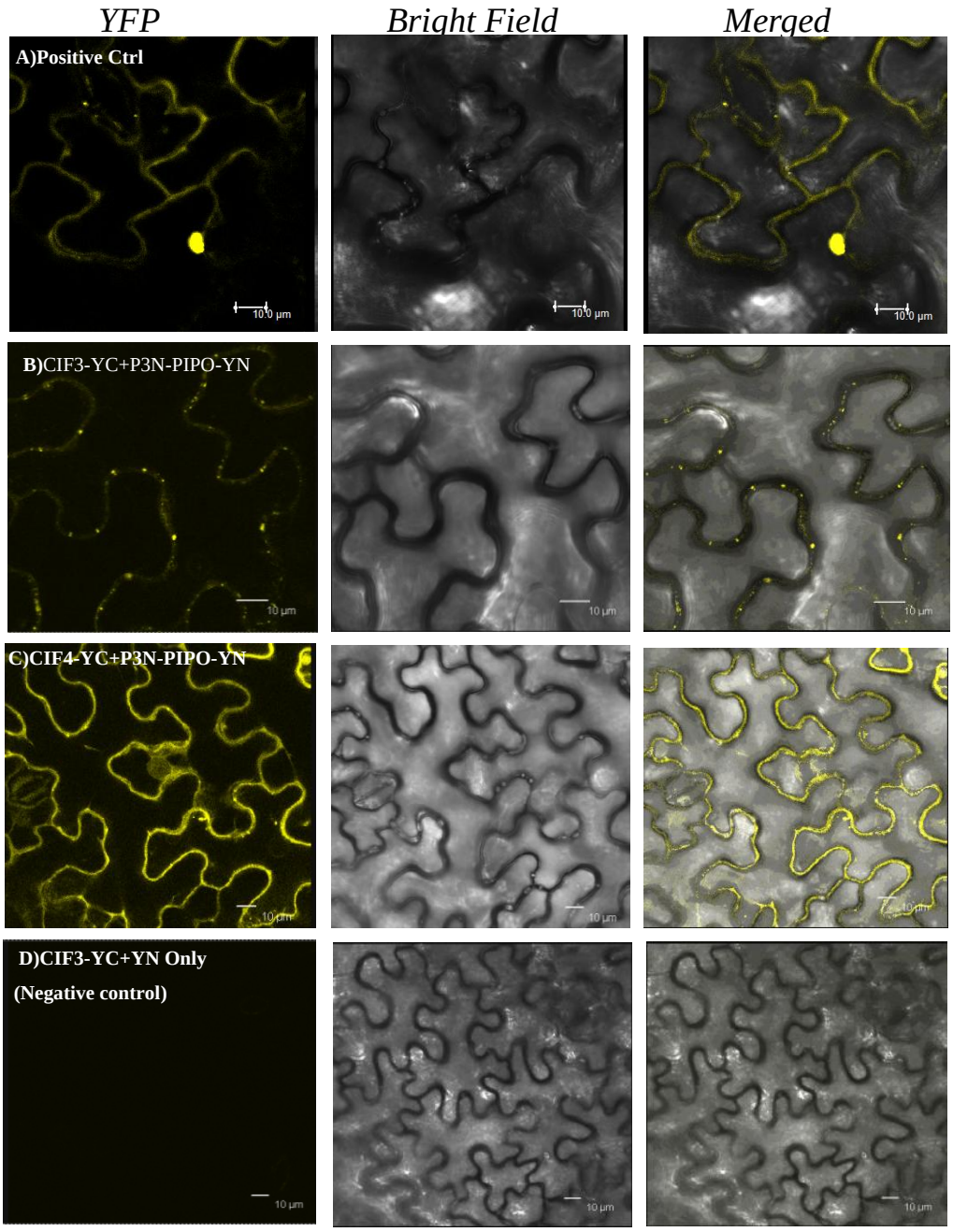

Figure 3.17 The N-terminal region of TuMV CI showed interactions with P3N-PIPO. Infiltrated *Nicotiana benthamiana* leaves were observed through a confocal microscope after two days post agroinfiltration. Scale bar 10 µm.

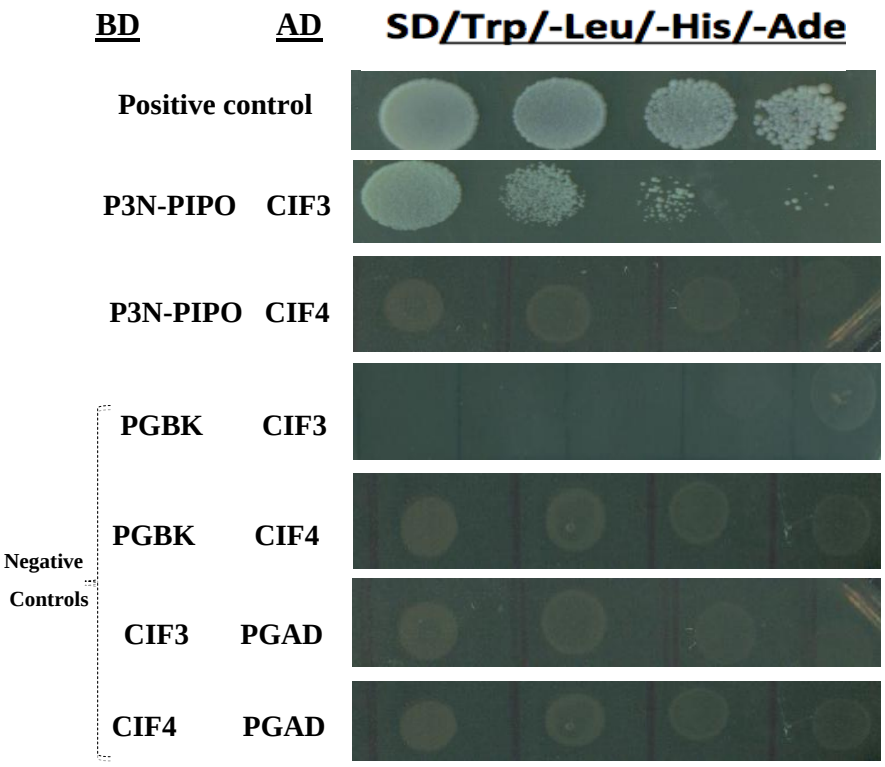

Figure 3.18 The CIF3 fragment of TuMV CI interacts with P3N-PIPO in the yeast two-hybrid assay. Ten-fold serial dilutions of cultures of yeast co-transformants were grown on the selective medium.

3.8 The N-terminal portion of TuMV CI protein is necessary for self-assembly

It is well known that CI interacts with CI (Sorel et al., 2014). To test what region(s) are responsible for CI self-interactions, the N- and C-terminal region regions (CIF1 and CIF2) of CI protein (1-334 aa) of TuMV BIFC assay *in planta* (Fig. 3.19) and Y2H assay in yeast (Fig. 3.20). The N-terminal region showed strong self-interactions in both assays. However, no positive self-interaction was found for the C-terminal region of CI protein either *in planta* or in yeast (Fig. 3.19 and 3.20).

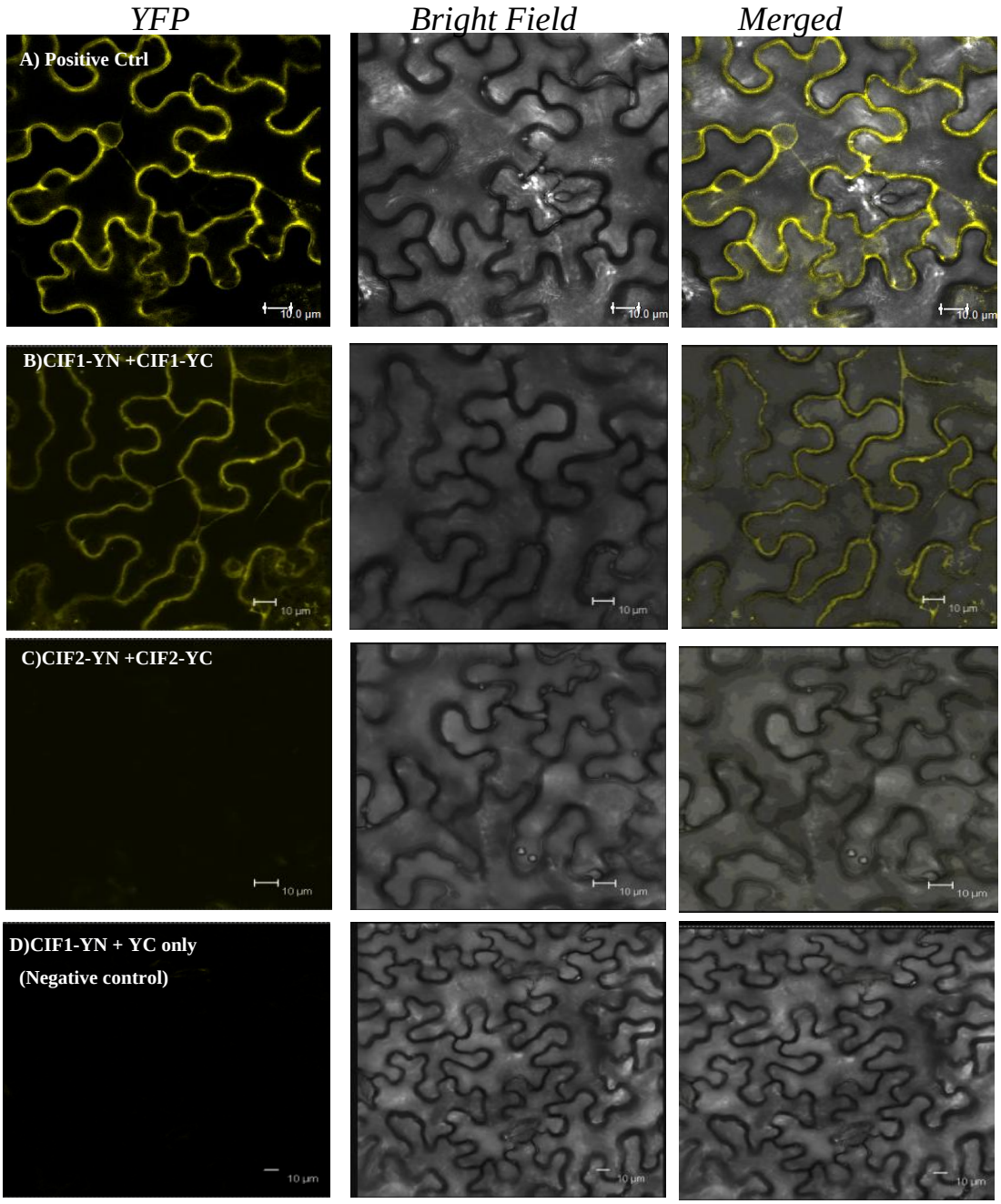

Figure 3.19 The N-terminal region of TuMV CI is responsible for the self-interaction *in planta*. BIFC self-interaction assay for positive control (A) N-terminal region (B), C-terminal region of TuMV CI (C) and negative control (D). Images were taken two days post inoculation. Scale bar 10 µm.

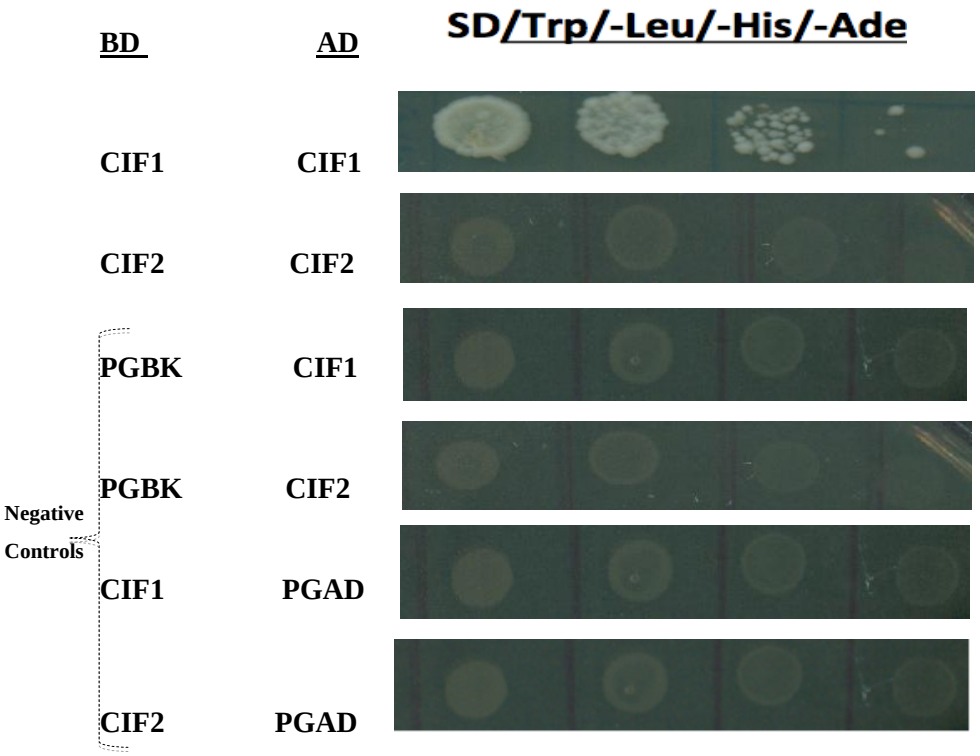

Figure 3.20 The N-terminal region of TuMV CI shows self-interaction in the yeast two-hybrid assay. CIF1 (1-334 aa), and CIF2 (335-644 aa) were examined individually for self-interaction. Ten-fold serial dilutions of cultures of yeast co-transformants were grown on the selective medium.

Chapter 4

4 Discussion

4.1 The potyviral P3N-PIPO protein is essential for intercellular movement

The cell-to-cell movement of potyviruses is composed of several ordinal steps including the elevated PD size exclusion limit, formation of the movement complex, viral intracellular transportation to and subsequent passage through the PD, and entry into the neighboring cell (Nelson and Citovsky, 2005; Benitez-Alfonso et al., 2010). This study was conducted to elucidate the functional roles of P3N-PIPO. My data showed that the introduction of a stop codon (TGA) to knock-out out the expression of the PIPO protein in TuMV impeded cell-to-cell movement and resulted in plants as healthy as un-inoculated ones and the negative control (Fig. 3.2 A, B and C). This finding is consistent with the results of several publications. Chung et al. (2008) discovered PIPO in potyviruses and reported that the introduction of stop codons in various places of PIPO is lethal for the TuMV life cycle (Chung et al., 2008). In an earlier study, Choi et al. (2005) reported *wheat streak mosaic virus* (WSMV) mutants containing the synonymous mutations in the C-terminal region of P3 lost the ability to infect plants systemically (Choi et al., 2005). In this study, I also provided evidence that the PIPO knock-out mutant that lost the ability for local movement remained competent for replication in *Nicotiana benthamiana* protoplast cells. Moreover, no systemic infection was detected in the upper newly emerging leaves of *Nicotiana benthamiana* seedlings inoculated by the PIPO knock-out mutant (Fig. 3.6). This result is consistent with the findings reported by Wen et al. (2010). They reported that SMV PIPO knock-out mutants, irrespective of

harboring one or multiple premature stop codons, were replication competent but restricted to small clusters of cells within the inoculated leaves (Wen et al., 2010). More recently, Geng et al. (2014) demonstrated that *Tobacco vein banding mosaic virus* (TVBMV) mutants expressing truncated PIPOs failed to move between cells and showed compromised systemic infection in the host plants (Geng et al., 2014). In addition to the PIPO knock-out mutant, I also generated several TuMV PIPO substitution mutants in which a positively charged residue (Lysine) at different positions was substituted with a negatively charged amino acid (Glutamic acid). These mutations were synonymous with respect to P3. Interestingly, like the PIPO knock-out mutant, these mutants lost the ability of cell-to-cell movement but viral replication was not affected (Fig. 3.5 and 3.7). It is possible that these substitutions change the structure of PIPO, leading to the loss of function. Similar substitution mutations in PIPO of SMV also compromised cell-to-cell movement of SMV without affecting SMV replication (Wen and Hajimorad, 2010). These data strongly support that the potyviral P3N-PIPO protein likely is a dedicated movement protein for potyviral intercellular movement.

4.2 Targeting the CI protein in PD is necessary for intercellular movement in potyviruses

Genetic and ultrastructural investigations in potyviruses revealed that cylindrical inclusion (CI) protein is involved in cell-to-cell spreading, likely through the formation of conical structures in the PD, a process that is mediated by P3N-PIPO (Wei et al., 2010). TuMV P3N-PIPO is a PD-located protein and its trafficking to PD requires the secretary pathway rather than the actomysoin motility system (Wei et al., 2010). In this study, I found that upon introduction of a stop codon to knock-out the expression of PIPO, the P3N lost the ability to accumulate to PD, and in the presence of this mutant, the TuMV

CI protein did not target to PD and instead was present in the cytoplasm (Fig. 3.11B). These data suggest the PIPO domain is essential for the localization of P3N-PIPO to PD as well as for tagerting of CI to PD.

Interestingly, although a substitution mutation at several different positively charged residues in TuMV P3N-PIPO did not affect PD-localization, these mutants lost the ability to move from cell-to-cell (Fig. 3.9). Transient coexpression of TuMV P3N-PIPO substitution mutants and CI revealed that they failed to target the CI protein to PD and the CI protein was apparently redistributed to the nucleus and cytoplasm (Fig3.12). The mechanism by which these P3N-PIPO substitution mutants are unable to mediate CI targeting to PD is not clear. Previous genetic analysis of TEV CI showed that a substitution affecting two aspartic residues at positions 3 and 4 of the CI protein disrupted the PD localization of CI, leading to an intercellular movement defective phenotype (Carrington et al., 1998; Wei et al., 2010). Taken together, these data suggest that trafficking of CI to PD is required for potyviral cell-to-cell movement and the PIPIO domain is essential in mediating this process.

4.3 P3N-PIPO anchors CI at PD likely via an indirect interaction with CI

Experimental Y2H data have been crucial for the evolution of protein interaction networks (Schwikowski et al., 2000; Uetz and Hughes, 2000) despite the limitation of yeast two-hybrid screens which can include non-specific or false interactions even with the most stringent screening conditions (Munder and Hinnen, 1999; Legrain and Selig, 2000; Brückner et al., 2009). This technique remains one of the most powerful methods and offers a sensitive and cost-effective mean to test the direct interaction between two

targeted proteins (Brückner et al., 2009). In this study I used the Y2H assay to determine if there is a direct interaction between TuMV P3N-PIPO and CI. The result was negative (Fig. 3.15). However, TuMV P3N-PIPO-YN and CI-YN showed a strong yellow fluorescence signal in the BIFC assay in *Nicothinia benthaminia* plants (Fig. 3.14B). This might suggest a possible indirect interaction between TuMV P3N-PIPO and CI proteins. Recently, PD was shown to to interact with the host protein PCaP1 (host hydrophilic cation binding protein) and knock-out of the PCaP1 expression significantly suppresses TuMV infection in *Nicotinia benthaminia* (Vijayapalani et al., 2012). It was speculated that PCaP1 links a complex of viral proteins and genomic RNA to the plasma membrane by binding P3N-PIPO, enabling localization to PD and cell-to-cell movement (Vijayapalani et al., 2012). However, it is not clear if PCaP1 binds to CI to bridge an indirect interaction between P3N-PIPO and CI. More recently, Geng et al. (2014) presented evidence showing that a developmentally regulated plasma membrane protein of *Nicotiana benthamiana*, referred to as NbDREPP, interacts with both the P3N-PIPO and CI of the *Tobacco vein banding mosaic virus* (TVBMV). Silencing of NbDREPP expression in *Nicothinia benthamiana* significantly impeded the viral spreading of TVBMV (Geng et al., 2014). Therefore, this protein might be a better candidate to build the link between P3N-PIPO and CI, although the recruitment of other host factors cannot be excluded.

4.4 The N-terminal region of TuMV CI protein is responsible for the interaction with P3N-PIPO and self-interaction

Previously, Carrington et al. provided evidence that most mutations in the N-terminal half of TEV CI protein affect virus spreading in tobacco plants (Carrington et al., 1998). In

this present work, I found that the N-terminal region of TuMV CI protein is a determinant domain for P3N-PIPO interaction *in planta* (Fig. 3.19). Moreover, I found a positive interaction between P3N-PIPO and the N-terminal fragment of TuMV CI protein (CIF1) in the Y2H assay. This is in contrast to my observation that no interaction was found between the full-length CI and P3N-PIPO in the yeast system (Fig. 3.16 and Fig. 3.11). As discussed earlier, host factor(s) may be involved in this process. For example, CI may interact with a host factor to expose the P3N-PIPO interacting domain in the N-terminal region that will make the interaction of P3N-PIPO and CI possible. It is also possible that there lacks a specific chaperone in yeast which assists the correct folding of viral proteins such as CI in comparison to plant cells. Therefore, truncated CI can be folded more easily in absence of the functional chaperone even without mediation of the specific host factor (Hartl et al., 2002).

Self-interaction was demonstrated *in planta* for the full-length CI protein of PPV and TEV by the BIFC assay (Wei et al., 2010; Zilian and Maiss, 2011). Targeting of TuMV CI to PD by P3N-PIPO may also be affected by CI self-interactions (Wei et al., 2010). Previously defective cell-to-cell movement CI mutants (DD3, 4AA and KK101, 102AA) in the N-terminal region of PPV, were shown to have reduced self-interacting strength and they were distributed to the cell periphery and the nucleus. Similar results were obtained from studies with PPV CI (Gomez de Cedron et al., 2006). In this study, I also found that the N-terminal region (177 amino acids of CI) is necessary for self-interaction (Fig. 3.19). In contrast to these findings, in the case of WSMV, the C-terminal region of the CI protein was shown to be responsible for self-interaction (Choi et al., 2005). Taken

together these data suggest that CI self-assembly is virus-specific and mutations that affect self-interaction abolish viral cell-to-cell movement (Sorel et al., 2014).

4.5 Conclusions and Prospective for Future Research

In this thesis, the involvement of TuMV P3N-PIPO protein in intercellular movement in *Nicotinia benthaminia* leaves' cells was assessed. I studied the effect of mutations in P3N-PIPO protein but synonymous in P3 on virus movement by using confocal microscopy and determined the ability of mutants to targeting CI protein to PD by subcellular co-localization. In addition, P3N-PIPO mutants were examined to see if viral replication is affected or not by PEG-mediated transfection assay in *Nicotinia benthaminia* protoplasts. The results revealed that insertion of stop codon and substitution mutations in PIPO ORF abolished viral intercellular movement and the mutated P3N-PIPO lost the ability to to target the CI protein to PD. My data also suggest that the mutation in P3N-PIPO do not affect viral replication. These findings strongly suggest that TuMV P3N-PIPO is a dedicated MP required for virus cell spreading. Further, the interaction of P3N-PIPO and CI, detected by BIFC was limited in PD and the extended CI structure inwards to the cytoplasm came from the CI-CI interaction without P3N-PIPO. This result suggests that P3N-PIPIO is an anchor protein to fix CI in PD and is in agreement with the previous observation that the CI protein is directly involved in cell-to-cell movement through the formation of cone-shaped structure anchored and extended through PD (Wei et al., 2010).

Viruses recruit host factors for their movement in plants (Raffaele et al., 2009; Amari et al., 2010; Ueki et al., 2010). The nature of host proteins contributing to cell-to-cell trafficking of potyvirus is poorly understood (Vijayapalani et al., 2012). In comparison to

the molecular characterization of MPs, not much work has been done to identify MP-interacting host proteins and understand their roles in viral intercellular movement (Geng et al., 2014). There are still many unanswered questions about the molecular mechanisms by which MPs and their interacting factor are delivered to PD (Harries et al., 2010). Therefore, the molecular identification of P3N-PIPO interacting host proteins and further characterization of their functional role in potyviral infection process will be one of the major research directions (Geng et al., 2014). Collectively, the knowledge obtained from this study has provided new insights into TuMV cell-to-cell movement. Since majority of potivral proteins are multifunctional proteins, it would also be interesting to examine other possible functions of P3N-PIPO such as the possible role in intracellular movement and the virulence determinant or symptom development factor (Choi et al., 2013; Hisa et al., 2014).

References

Adams MJ, Antoniw JF, Beaudoin F (2005) Overview and analysis of the polyprotein cleavage sites in the family Potyviridae. Mol Plant Pathol **6:** 471-487.

Agbeci M, Grangeon R, Nelson RS, Zheng H, Laliberté J-F (2013) Contribution of host intracellular transport machineries to intercellular movement of turnip mosaic virus. PLoS pathog **9:** e1003683.

Ahlquist P, Noueiry AO, Lee WM, Kushner DB, Dye BT (2003) Host factors in positive-strand RNA virus genome replication. J Virol **77:** 8181-8186.

Amari K, Boutant E, Hofmann C, Schmitt-Keichinger C, Fernandez-Calvino L, Didier P, Lerich A, Mutterer J, Thomas CL, Heinlein M (2010) A family of plasmodesmal proteins with receptor-like properties for plant viral movement proteins. PLoS pathog **6:** e1001119.

Benitez-Alfonso Y, Faulkner C, Ritzenthaler C, Maule AJ (2010) Plasmodesmata: gateways to local and systemic virus infection. Mol Plant Microbe Interact **23:** 1403-1412.

Blanc S, Lopez-Moya JJ, Wang R, Garcia-Lampasona S, Thornbury DW, Pirone TP (1997) A specific interaction between coat protein and helper component correlates with aphid transmission of a potyvirus. Virol **231:** 141-147.

Boevink P, Oparka KJ (2005) Virus-host interactions during movement processes. Plant Physiol **138:** 1815-1821.

Brückner A, Polge C, Lentze N, Auerbach D, Schlattner U (2009) Yeast two-hybrid, a powerful tool for systems biology. Int J Mol Sci **10:** 2763-2788.

Carrington JC, Jensen PE, Schaad MC (1998) Genetic evidence for an essential role for potyvirus CI protein in cell-to-cell movement. Plant J **14:** 393-400.

Choi IR, Horken KM, Stenger DC, French R (2005) An internal RNA element in the P3 cistron of Wheat streak mosaic virus revealed by synonymous mutations that affect both movement and replication. J Gen Virol **86:** 2605-2614.

Choi SH, Hagiwara-Komoda Y, Nakahara KS, Atsumi G, Shimada R, Hisa Y, Naito S, Uyeda I (2013) Quantitative and qualitative involvement of P3N-PIPO in overcoming recessive resistance against Clover yellow vein virus in pea carrying the cyv1 gene. Virol **87:** 7326-7337.

Chung BY, Miller WA, Atkins JF, Firth AE (2008) An overlapping essential gene in the Potyviridae. Proc Natl Acad Sci U S A **105:** 5897-5902.

Chung WY, Wadhawan S, Szklarczyk R, Pond SK, Nekrutenko A (2007) A first look at ARFome: dual-coding genes in mammalian genomes. PLoS Comput Biol **3:** e91.

Cotton S, Grangeon R, Thivierge K, Mathieu I, Ide C, Wei T, Wang A, Laliberte JF (2009) Turnip mosaic virus RNA replication complex vesicles are mobile, align with microfilaments, and are each derived from a single viral genome. J Virol **83:** 10460-10471.

Culley AI, Lang AS, Suttle CA (2003) High diversity of unknown picorna-like viruses in the sea. Nature **424:** 1054-1057.

Dreher TW, Miller WA (2006) Translational control in positive strand RNA plant viruses. Virol **344:** 185-197.

Dunoyer P, Thomas C, Harrison S, Revers F, Maule A (2004) A cysteine-rich plant protein potentiates Potyvirus movement through an interaction with the virus genome-linked protein VPg. Virol **78:** 2301-2309.

Fauquet CM, Mayo M, Maniloff J, Desselberger U, Ball LA (2005) Virus taxonomy: VIIIth report of the International Committee on Taxonomy of Viruses. Elsevier Academic Press. Amsterdam.

Fellers J, Wan J, Hong Y, Collins GB, Hunt AG (1998) In vitro interactions between a potyvirus-encoded, genome-linked protein and RNA-dependent RNA polymerase. J Gen Virol **79 (Pt 8):** 2043-2049.

Fernandez-Fernandez MR, Martinez-Torrecuadrada JL, Roncal F, Dominguez E, Garcia JA (2002) Identification of immunogenic hot spots within plum pox potyvirus capsid protein for efficient antigen presentation. J Virol **76:** 12646-12653.

Geng C, Cong Q-Q, Li X-D, Mou A, Gao R, Liu J, Tian Y (2014) NbDREPP Contributes to Potyvirus Movement and Transports to Plasmodesmata via the Early Secretory Pathway and the Actomyosin System. Plant physiol **167.2**:394-410.

Gergerich RC, Dolja VV (2006) Introduction to plant viruses, the invisible foe. The Plant Health Instructor. doi: 10.1094/PHI-I-2006-0414-01.

Gomez de Cedron M, Osaba L, Lopez L, Garcia JA (2006) Genetic analysis of the function of the plum pox virus CI RNA helicase in virus movement. Virus Res **116:** 136-145.

Grangeon R, Jiang J, Wan J, Agbeci M, Zheng H, Laliberté J-F (2013) 6K2-induced vesicles can move cell to cell during turnip mosaic virus infection. Front Microbiol **4:**351. doi:10.3389/fmicb.2013.00351.

Harries P, Ding B (2011) Cellular factors in plant virus movement: at the leading edge of macromolecular trafficking in plants. Virol **411:** 237-243.

Harries PA, Schoelz JE, Nelson RS (2010) Intracellular transport of viruses and their components: utilizing the cytoskeleton and membrane highways. Mol Plant Microbe Interact **23:** 1381-1393.

Heinlein M (2015) Plasmodesmata: Channels for Viruses on the Move. Methods Mol. Biol **1217:** 25–52.

Hillung J, Elena SF, Cuevas JM (2013) Intra-specific variability and biological relevance of P3N-PIPO protein length in potyviruses. BMC Evol Biol **13:** 249.

Hipper C, Brault V, Ziegler-Graff V, Revers F (2013) Viral and cellular factors involved in phloem transport of plant viruses. Front Plant Sci **4:**154. doi:10.3389/fpls.2013.00154.

Hisa Y, Suzuki H, Atsumi G, Choi SH, Nakahara KS, Uyeda I (2014) P3N-PIPO of Clover yellow vein virus exacerbates symptoms in pea infected with White clover mosaic virus and is implicated in viral synergism. Virol **449:** 200-206.

Hofius D, Maier AT, Dietrich C, Jungkunz I, Bornke F, Maiss E, Sonnewald U (2007) Capsid protein-mediated recruitment of host DnaJ-like proteins is required for Potato virus Y infection in tobacco plants. J Virol **81:** 11870-11880.

Hull R (2013) Plant virology. Academic press. San Diego CA.

Ivanov KI, Eskelin K, Lõhmus A, Mäkinen K (2014) Molecular and cellular mechanisms underlying potyvirus infection. J Gen Virol **95:** 1415-1429.

James P, Halladay J, Craig EA (1996) Genomic libraries and a host strain designed for highly efficient two-hybrid selection in yeast. Genetics **144:** 1425-1436.

Jebasingh T, Pandaranayaka EP, Mahalakshmi A, Kasin Yadunandam A, Krishnaswamy S, Usha R (2013) Expression, purification and molecular modeling of the NIa protease of Cardamom mosaic virus. J Biomol Struct Dyn **31:** 602-611.

King AM, Adams MJ, Lefkowitz EJ, Carstens EB (2012) Virus taxonomy: classification and nomenclature of viruses: Ninth Report of the International Committee on Taxonomy of Viruses, Elsevier, Academic Press, London, UK.

Laliberté J-F, Sanfaçon H (2010) Cellular remodeling during plant virus infection. Annu Rev Plant Physiol **48:** 69-91.

Legrain P, Selig L (2000) Genome-wide protein interaction maps using two-hybrid systems. FEBS letters **480:** 32-36.

López-Moya JJ, Valli A, García JA (2009) Potyviridae. In: Encyclopedia of Life Sciences (ELS). John Wiley & Sons, Ltd., Chichester,U.K. doi:10.1002/9780470015902.

Lu Q, Tang X, Tian G, Wang F, Liu K, Nguyen V, Kohalmi SE, Keller WA, Tsang EW, Harada JJ, Rothstein SJ, Cui Y (2010) Arabidopsis homolog of the yeast TREX-2 mRNA export complex: components and anchoring nucleoporin. Plant J **61:** 259-270.

Lucas WJ (2006) Plant viral movement proteins: agents for cell-to-cell trafficking of viral genomes. Virol **344:** 169-184.

Majer E, Salvador Z, Zwart MP, Willemsen A, Elena SF, Daròs J-A (2014) Relocation of the NIb gene in the tobacco etch potyvirus genome. Virol **88:** 4586-4590.

Mallory AC, Ely L, Smith TH, Marathe R, Anandalakshmi R, Fagard M, Vaucheret H, Pruss G, Bowman L, Vance VB (2001) HC-Pro suppression of transgene silencing eliminates the small RNAs but not transgene methylation or the mobile signal. Plant Cell **13:** 571-583.

Matthews REF, Hull R (2002) Matthews' plant virology. Gulf Professional Publishing. Norwich UK.

Munder T, Hinnen A (1999) Yeast cells as tools for target-oriented screening. Appl Microbiol Biotechnol **52:** 311-320.

Nagy PD, Pogany J (2012) The dependence of viral RNA replication on co-opted host factors. Nat Rev Microbiol **10:** 137-149.

Nelson RS, Citovsky V (2005) Plant viruses. Invaders of cells and pirates of cellular pathways. Plant physiol **138:** 1809-1814.

Nguyen HD, Tomitaka Y, Ho SY, Duchêne S, Vetten H-J, Lesemann D, Walsh JA, Gibbs AJ, Ohshima K (2013) Turnip mosaic potyvirus probably first spread to Eurasian Brassica crops from wild orchids about 1000 years ago. PloS one **8:** e55336.

Ohshima K, Yamaguchi Y, Hirota R, Hamamoto T, Tomimura K, Tan Z, Sano T, Azuhata F, Walsh JA, Fletcher J (2002) Molecular evolution of Turnip mosaic virus: evidence of host adaptation, genetic recombination and geographical spread. J Gen Virol **83:** 1511-1521.

Oparka KJ (2004) Getting the message across: how do plant cells exchange macromolecular complexes? Trends Plant Sci **9:** 33-41.

Raffaele S, Bayer E, Lafarge D, Cluzet S, Retana SG, Boubekeur T, Leborgne-Castel N, Carde J-P, Lherminier J, Noirot E (2009) Remorin, a solanaceae

protein resident in membrane rafts and plasmodesmata, impairs potato virus X movement. Plant Cell **21:** 1541-1555.

Riechmann JL, Lain S, Garcia JA (1992) Highlights and prospects of potyvirus molecular biology. J Gen Virol **73 (Pt 1):** 1-16.

Rodamilans B, Valli A, Mingot A, San León D, Baulcombe D, López-Moya JJ, García JA (2015) RNA polymerase slippage as a mechanism for the production of frameshift gene products in plant viruses of the Potyviridae family. J Virol. doi:10.1128/JVI.00337-15.

Roudet-Tavert G, German-Retana S, Delaunay T, Delécolle B, Candresse T, Le Gall O (2002) Interaction between potyvirus helper component-proteinase and capsid protein in infected plants. J Gen Virol **83:** 1765-1770.

Saenz P, Cervera MT, Dallot S, Quiot L, Quiot JB, Riechmann JL, Garcia JA (2000) Identification of a pathogenicity determinant of Plum pox virus in the sequence encoding the C-terminal region of protein P3+6K(1). J Gen Virol **81:** 557-566.

Sambrook, J., and Russell, D.W. (2006) The condensed protocols from molecular cloning: a laboratory manual. (Cold Spring Harbor, NY: Cold Spring Harbor Laboratory Press)

Sánchez F, Martínez-Herrera D, Aguilar I, Ponz F (1998) Infectivity of turnip mosaic potyvirus cDNA clones and transcripts on the systemic host Arabidopsis thaliana and local lesion hosts. Virus Res **55:** 207-219.

Scholthof K-BG (2008) Tobacco Mosaic Virus: The Beginning of Plant Virology. APSnet Features. doi: 10.1094/APSnetFeatures-2008-2009.

Schwikowski B, Uetz P, Fields S (2000) A network of protein–protein interactions in yeast. Nature Biotechnol **18:** 1257-1261.

Shukla DD, Ward CW, Brunt AA (1994) The Potyviridae. Cab International. Wallingford, UK. doi: 10.1111/j.1469-8137.

Simon AE, Miller WA (2013) 3′ Cap-independent translation enhancers of plant viruses. Annu Rev Microbio **67:** 21.

Sorel M, Garcia JA, German-Retana S (2014) The Potyviridae cylindrical inclusion helicase: a key multipartner and multifunctional protein. Mol Plant Microbe Interact **27:** 215-226.

Syller J (2006) The roles and mechanisms of helper component proteins encoded by potyviruses and caulimoviruses. Physiol Mol Plant Path **67:** 119-130.

Taliansky M, Torrance L, Kalinina NO (2008) Role of plant virus movement proteins. Methods Mol Biol **451:**33-54.

Tena Fernández F, González I, Doblas P, Rodríguez C, Sahana N, Kaur H, Tenllado F, Praveen S, Canto T (2013) The influence of cis-acting P1 protein and translational elements on the expression of Potato virus Y helper-component proteinase (HCPro) in heterologous systems and its suppression of silencing activity. Mol Plant Pathol **14:** 530-541.

Thresh J (2006) Crop viruses and virus diseases: a global perspective. In Virus Diseases and Crop Biosecurity. doi: 10.1007/978-1-4020-5298-9-2.

Tomlinson J (1987) Epidemiology and control of virus diseases of vegetables. Ann Appl Biol **110:** 661-681.

Torres-Barceló C, Daròs J-A, Elena SF (2010) Compensatory molecular evolution of HC-Pro, an RNA-silencing suppressor from a plant RNA virus. Mol Biol Evol **27:** 543-551.

Ueki S, Spektor R, Natale DM, Citovsky V (2010) ANK, a host cytoplasmic receptor for the Tobacco mosaic virus cell-to-cell movement protein, facilitates intercellular transport through plasmodesmata. PLoS pathog **6:** e1001201.

Uetz P, Hughes RE (2000) Systematic and large-scale two-hybrid screens. Curr Opin Microbiol **3:** 303-308.

Urcuqui-Inchima S, Haenni AL, Bernardi F (2001) Potyvirus proteins: a wealth of functions. Virus Res **74:** 157-175.

van Regenmortel MH, Fauquet C, Bishop D, Carstens E, Estes M, Lemon S, Maniloff J, Mayo M, McGeoch D, Pringle C (2000) Virus taxonomy: classification and nomenclature of viruses. Seventh report of the International Committee on Taxonomy of Viruses. Academic Press. San Diego, CA.

Vijayapalani P, Maeshima M, Nagasaki-Takekuchi N, Miller WA (2012) Interaction of the trans-frame potyvirus protein P3N-PIPO with host protein PCaP1 facilitates potyvirus movement. PLoS Pathog **8:** e1002639.

Walsh JA, Jenner CE (2002) Turnip mosaic virus and the quest for durable resistance. Mol Plant Pathol **3:** 289-300.

Wei T, Wang A (2008) Biogenesis of cytoplasmic membranous vesicles for plant potyvirus replication occurs at endoplasmic reticulum exit sites in a COPI- and COPII-dependent manner. J Virol **82:** 12252-12264.

Wei T, Zhang C, Hong J, Xiong R, Kasschau KD, Zhou X, Carrington JC, Wang A (2010) Formation of complexes at plasmodesmata for potyvirus intercellular movement is mediated by the viral protein P3N-PIPO. PLoS Pathog **6:** e1000962.

Wei T, Zhang C, Hou X, Sanfacon H, Wang A (2013) The SNARE protein Syp71 is essential for turnip mosaic virus infection by mediating fusion of virus-induced vesicles with chloroplasts. PLoS Pathog **9:** e1003378.

Wen RH, Hajimorad MR (2010) Mutational analysis of the putative pipo of soybean mosaic virus suggests disruption of PIPO protein impedes movement. Virol **400:** 1-7.

Wu FH, Shen SC, Lee LY, Lee SH, Chan MT, Lin CS (2009) Tape-Arabidopsis Sandwich - a simpler Arabidopsis protoplast isolation method. Plant Methods **5:** 16.

Xiong R, Wang A (2013) SCE1, the SUMO-conjugating enzyme in plants that interacts with NIb, the RNA-dependent RNA polymerase of Turnip mosaic virus, is required for viral infection. J Virol **87:** 4704-4715.

Zilian E, Maiss E (2011) Detection of plum pox potyviral protein–protein interactions in planta using an optimized mRFP-based bimolecular fluorescence complementation system. J Gen Virol **92:** 2711-2723.

Appendices:

Appendix A: List of all the interactions tested by BIFC*

YN/YC	P3N-PIPO	PIPO (R9St)	PIPO (K15E)	PIPO (K28E)	PIPO (K41E)	CI	CIF1	CIF2	CIF3	CIF4
P3N-PIPO						+ PD	+ C	–	+ PD	+ N,C
PIPO (R9St)						–				
PIPO (K15E)						–				
PIPO (K28E)						–				
PIPO (K41E)						–				
CI	+ PD	–	–	–	–	+ C,N				
CIF1	+ C									
CIF2	–									
CIF3	+ PD									
CIF4	+ N,C									

*YN, protein fused to N-terminal YFP; -YC, protein fused to C-terminal YFP, N-Nucleus; C-cytoplasm, PD-plasmodesmata.

Appendix B: List of all the interactions tested by Y2H*

AD/BD	P3N-PIPO	PIPO (K15E)	PIPO (K28E)	PIPO (K41E)	CI	PGBKT7
P3N-PIPO					–	–
PIPO (K15E)					–	–
PIPO (K28E)					–	–
PIPO (K41E)					–	–
CI	–	–	–	–		–
PGADT7	–	–	–	–	–	–

*BD-, protein fused to Gal4 binding domain; AD-, protein fused to Gal4 activation domain; pGADT7 & pGBKT7, empty vectors for Y2H.

Curriculum Vitae

Name:	Hoda Yaghmaiean
Post-secondary Education and Degrees:	The University of Tehran Tehran, Iran 2003-2007 (Microbiology B.A). The University of Tehran Tehran, Iran 2007-2010 (Microbiology M.Sc). The University of Western Ontario London, Ontario, Canada 2013-2015 (Molecular biology & Virology M.Sc).
Honours and Awards:	Western Graduate Research Scholarship (WGRS) 2013-2015.
Related Work Experience	Teaching Assistant The University of Western Ontario 2013-2015

Publications:

Yaghmaiean H, Fazeli M, Jamalifar H, Ilka H, Tagavian M. (2012). Propagation of Encephalomyocarditis virus particles in A549 and L929 cell lines, Iranian Journal of Microbiology, 5(3), 29-37.

Yaghmaiean H, Ghavamzadeh H and Alimoghadam K. (2008). Freezing Cord Blood Stem Cells report across two years 2008-2009. 8th International Conference on Haematology and Oncology, October 7-10, 2008.Oromia, Iran.